ORNL/TM-6781

Use of Ultimate Tensile Strength to Estimate the Creep-Rupture Behavior of Austenitic Weld Metals and Castings

V. K. Sikka
J. W. McEnerney

OAK RIDGE NATIONAL LABORATORY
OPERATED BY UNION CARBIDE CORPORATION · FOR THE DEPARTMENT OF ENERGY

ORNL/TM-6781
Distribution
Category
UC-79b, -h, -k

Contract No. W-7405-eng-26
METALS AND CERAMICS DIVISION

USE OF ULTIMATE TENSILE STRENGTH TO ESTIMATE THE CREEP-RUPTURE BEHAVIOR OF AUSTENITIC WELD METALS AND CASTINGS

V. K. Sikka and J. W. McEnerney

Date Published: May 1979

OAK RIDGE NATIONAL LABORATORY
Oak Ridge, Tennessee 37830
operated by
UNION CARBIDE CORPORATION
for the
DEPARTMENT OF ENERGY

Blank Page

CONTENTS

USE OF ULTIMATE TENSILE STRENGTH TO ESTIMATE THE CREEP-RUPTURE BEHAVIOR OF AUSTENITIC WELD METALS AND CASTINGS*

V. K. Sikka and J. W. McEnerney

ABSTRACT

Nuclear and fossil power plants, coal conversion systems, and chemical plants constructed of types 304 and 316 stainless steel generally contain welds deposited with type 308, 316, or 16-8-2 filler metal. Autogenous welds (without filler metal) may also be used. Creep data from weld metal are in short supply and, when available, typically show large variations due to the complex microstructure resulting from welding process variables. The scatter in the weld metal data has made data analysis rather difficult. However, we show prospects for estimating weld creep data with significant success by use of knowledge of weld metal elevated-temperature tensile properties. Previously developed base metal rupture time and minimum creep rate empirical models containing an elevated-temperature ultimate tensile strength are extended to the weld metal data.

We applied the base-metal models for type 304 stainless steel to type 308 weld metal and models for type 316 to type 316 or 16-8-2 weld metal. The data analyzed were to both as-welded and heat-treated weld metals and weldments, centrifugally cast pipes, and the riser portions of static castings of types 316L and 316 stainless steel. The weldments investigated were made by the submerged-arc, shielded metal-arc, and gas tungsten-arc processes. The data on castings were analyzed both as cast and after sigma heat-treatment. Creep-rupture tests extending over rupture times ranging to 10,000 h and temperatures from 482 to 649°C were considered.

We concluded that elevated-temperature ultimate tensile strength can be used as a possible *index* for estimating the creep-rupture time and minimum creep rate properties of austenitic welds and castings. The rupture times were generally predicted more accurately than the minimum creep rates. The use of elevated-temperature ultimate tensile strength is also suggested to check if the fabrication procedures during welding are followed and if the weldment meets the specified creep properties.

---

*Work performed under DOE/RRT 189s OH024, Joining Technology Development; OH050, Mechanical Properties for Structural Materials; and OH103, Piping and Fittings Development.

INTRODUCTION

Nuclear and fossil power plants, coal conversion systems, and chemical plants all contain welds that must operate over a range of temperatures, stresses, and environments. These welds are present in a variety of systems or components such as piping, pressure vessels, and support structures. Austenitic stainless steels (types 304 and 316) are typically used for systems that operate in the creep range, 427 to 649°C. Systems constructed of types 304 and 316 stainless steel generally contain welds deposited with types 308, 316, and 16-8-2 filler metals. However, autogenous welds (without filler metal) may also be used. Creep data from weld metal are in short supply and, when available, typically show large variations due to the complex microstructure of the weld metal, which results from welding process variables such as filler metal and flux composition, arc atmosphere composition, dilution, heat input, and welding travel speed. The scatter in the weld metal data has made the task of data analysis rather difficult in the past. However, our recent work has given some prospects for estimating the weld creep data with significant success from a knowledge of weld metal elevated-temperature tensile properties. The present method involves extending previously developed[1,2] base metal empirical models to treating the weld metal data.

The purpose of this report is to show how the base metal models can be extended to predict the weld metal properties by using the appropriate elevated-temperature ultimate tensile strength of the weld metal. The predicting capabilities will be checked for all time-to-rupture and minimum creep rate data available from the literature. The present analysis will also be extended to some results on as-cast types 304 and 316 stainless steel.

METHODS OF ANALYSIS

The previously developed[1,2] models for base metal predict time to rupture (t_r) and minimum creep rate ($\dot{\varepsilon}_m$) from a knowledge of stress (σ),

temperature (T), and ultimate tensile strength (S_u) at the creep test temperature and a fixed strain rate. The models were of the form

$$t_r \text{ or } \dot{\varepsilon}_m = f(\sigma, T, \text{ and } S_u) \ . \tag{1}$$

In the base metal analysis S_u was used to describe the creep behavior of an individual heat. Since the weld metal is generally of different composition and microstructure than the base metal, it can therefore be considered as a different heat of material than the base metal. Thus, it should be possible to extend the base metal models to describe the creep-rupture behavior of the weld metal by using its appropriate elevated-temperature ultimate tensile strength.

We also assume in this report that the base metal models for type 304 can be applied to type 308 weld metal and models for type 316 can be applied to type 316 or 16-8-2 weld metal. This assumption is based on similarities in chemical analysis of types 304 and 308 and types 316 and 16-8-2 weld metal. The previously published[1] base metal models without S_u (to represent the average behavior) and with S_u (to predict the behavior of individual heats) are given by the following equations:

Type 304

Time to Rupture (t_r, h)

without S_u —

$$\log t_r = 31.196 - 4.0918 \log \sigma - 8.497 \times 10^{-3}\sigma - 2.0056 \times 10^{-2}T \tag{2}$$

with S_u —

$$\log t_r = 4.5283 + \frac{13.0S_u}{T} + \frac{16142}{T} - \frac{6328.6}{T} \log \sigma \tag{3}$$

Minimum Creep Rate ($\dot{e}_m$, %/h)

without S_u —

$$\log \dot{e}_m = 23.503 + \frac{7873.9 \log \sigma}{T} - \frac{39825}{T} \tag{4}$$

with S_u —

$$\log \dot{e}_m = 7.6618 - \frac{15.281S_u}{T} - \frac{19298}{T} + \frac{7161.7}{T} \log \sigma \qquad (5)$$

with σ and S_u in MPa and T in K.

Type 316

Time to Rupture (t_r, h)

without S_u —

$$\log t_r = -7.801 - 3.047 \log \sigma - 0.009098\sigma + \frac{17565}{T} \qquad (6)$$

with S_u —

$$\log t_r = -5.138 - 2.181 \log \sigma + \frac{13768}{T} - \frac{3771\sigma}{TS_u} \qquad (7)$$

Minimum Creep Rate ($\dot{e}_m$, %/h)

without S_u —

$$\log \dot{e}_m = 9.6223 + 4.592 \log \sigma + 0.00725\sigma - \frac{21120}{T} \qquad (8)$$

with S_u —

$$\log \dot{e}_m = -3.534 + 2.0734 \log \sigma - \frac{45.064S_u}{T} + 0.01836S_u \log \sigma \qquad (9)$$

with σ and S_u in MPa and T in K.

Models for both types were based on data collected from the literature[3] in which elevated-temperature S_u values were specified. The S_u values in Eqs. (3), (5), (7), and (9) were at a strain rate of 8.33×10^{-5}/s (0.00500/min). The number of data points for deriving t_r and $\dot{e}_m$ models for type 304 stainless steel were 146 and 82, respectively. For type 316 there were 132 and 102 data points, respectively.

The models without S_u represent an average base model behavior, whereas models with S_u predict the behavior of an individual weld by substitution of its S_u value at the creep test temperature.

The following sections compare the predicted curves and the experimental results for various data sources. The data analyzed were obtained from transverse [composite weld metal, heat-affected zone (HAZ) and base metal] and longitudinal (all weld metal) specimens from types 308, 16-8-2, 316, and autogenous welds. These welds were made by the submerged-arc, shielded metal-arc, and gas tungsten-arc processes. The welds were in the following heat-treated conditions: as-welded, heated in the "885°F embrittlement" range, heated in the sigma range, and solution annealed. Each data source will be treated separately. These comparisons will be followed by a general discussion section.

RESULTS

Babcock and Wilcox 16-8-2 Submerged-Arc Welds (ORNL Data[4])

These data are on 16-8-2 trial welds made by Babcock and Wilcox (B&W). The submerged-arc process was used in a 25-mm-thick type 316 stainless steel plate. The welds were made in a single V-joint with a 19-mm root opening and a 20° included angle. Arcos S-11 Flux was used. All the tensile and creep tests were performed on these welds by King et al.[4] at ORNL. Predictions and experimental data for these 16-8-2 welds are compared in Figs. 1 and 2. The letters L_1 and L_2 in these figures represent longitudinal specimens from the crown and root, respectively, of the weld. The letter T_1 represents the transverse specimen from the crown of the weld. Figure 1 also includes the ASME Code Case N-47 minimum stress-rupture curve[5] for the base metal. This figure shows that the 16-8-2 weld metal (L_1) data were not only significantly below the average values for the base metal but also below the Code Case minimum curve.

Figures 1 and 2 show that the curves predicted by using the elevated-temperature S_u values describe the experimental data well at

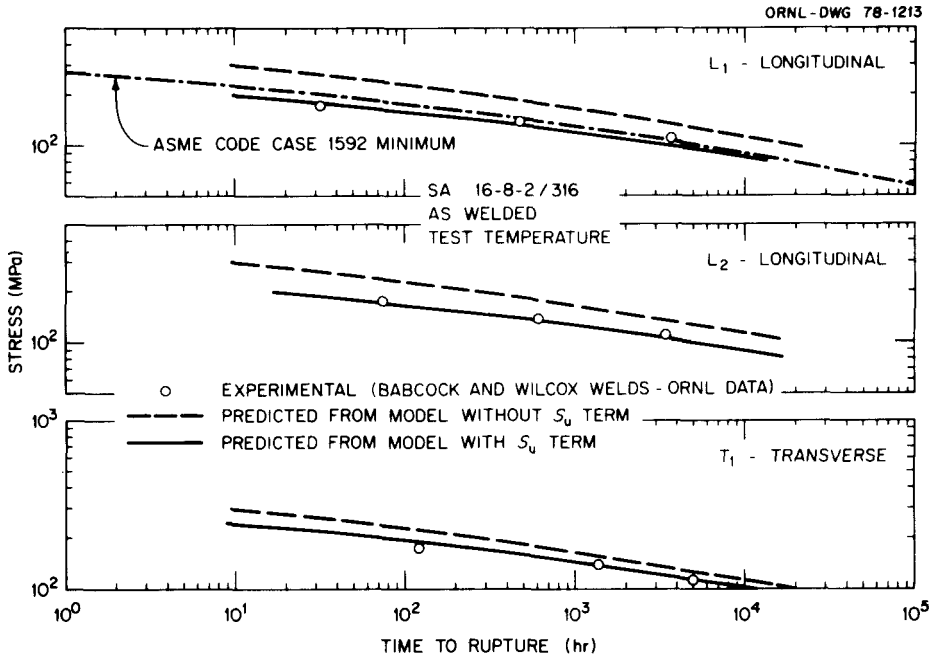

Fig. 1. Comparison of Experimental Time to Rupture with Values Computed from Models with and without Elevated-Temperature S_u for Submerged-Arc 16-8-2 Weld Metal at 649°C (King et al. Data). Also shown is the ASME Code Case N-47 (formerly 1592) minimum.

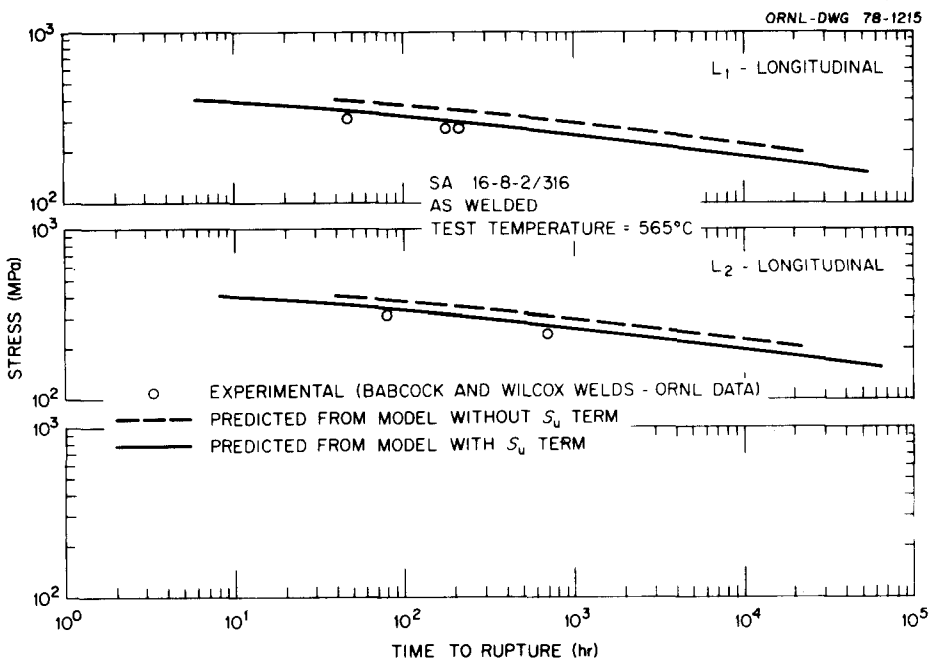

Fig. 2. Comparison of Experimental Time to Rupture with Values Computed from Models with and without Elevated-Temperature S_u for Submerged-Arc 16-8-2 Weld Metal at 565°C (King et al. Data).

both 649 and 565°C. Note also that the proper S_u values can even predict the difference in creep properties between the crown and root of the weld in the longitudinal direction and between the longitudinal and transverse directions in the crown of the weld. It should be pointed out that the longest test time on the submerged-arc welds was only 5000 h. The ferrite content in B&W welds ranged from 0.8 to 3.0 in ferrite number (FN). Although the predicted values from rupture models containing elevated-temperature ultimate tensile strength describe the short-term data very well, we recommend that these models not be used to extrapolate beyond the range of available test times. The same restriction is also true for the creep data plotted in the remaining figures of this report.

SMA and GTA 16-8-2 Welds (King et al.[6])

These data are on seven different 16-8-2 welds. All the welds were made in 12.7-mm-thick plates from a single heat of material. All the filler metals were deposited in V-groove butt joints having a 75° included angle, a 1.6-mm root gap, and a 0.38-mm minimum root face. The plates were restrained from flexing about the weld but were free to move in the plane of the plate. The welding conditions are given in Table 2 of ref. 6. The welds V-03 and V-04 were made by the shielded metal-arc (SMA) process, whereas all other welds were made by the gas tungsten-arc (GTA) process. The welds V-66 to V-74 were made by the automatic process whereas all other welds were made by the manual process.

Predictions and experimental data for these welds are compared in Figs. 3 through 5. Figures 3 and 4 show comparisons for various welds at 649°C, and Fig. 5 shows comparisons for welds V-66 through V-74 at three different test temperatures, 482, 593, and 649°C. The t_r data for all welds at 649°C (Figs. 3 and 4) were below the average value curve predicted for the base metal and could be predicted closely by the model containing elevated-temperature S_u, Eq. (7).

Although the t_r values for various welds were lower than the average value curve for the base metal, the $\dot{e}_m$ values on the same

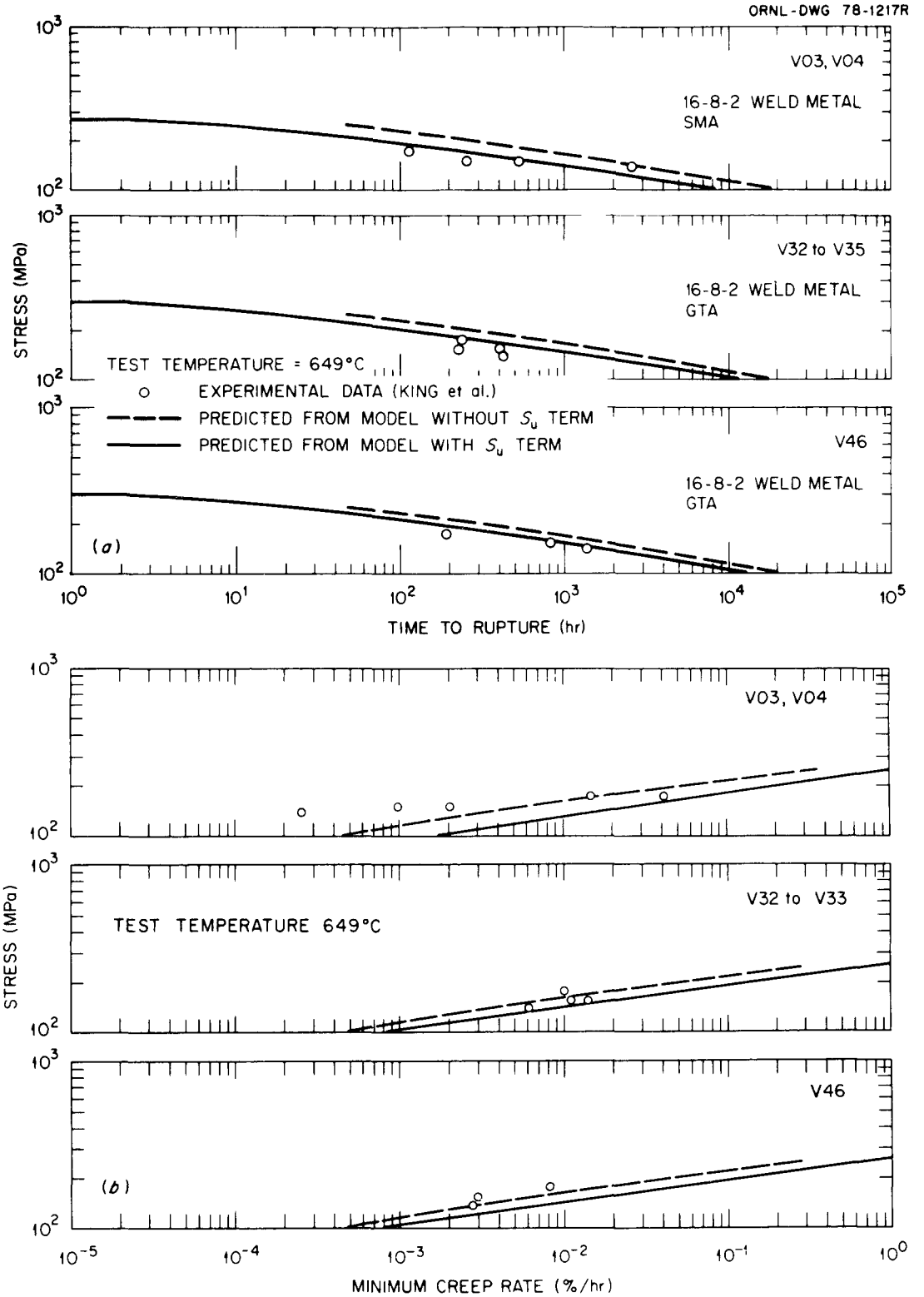

Fig. 3. Comparison of Experimental Time to Rupture and Minimum Creep Rate with Values Computed from Models with and without Elevated-Temperature S_u for SMA and GTA 16-8-2 Welds at 649°C (King et al. Data).

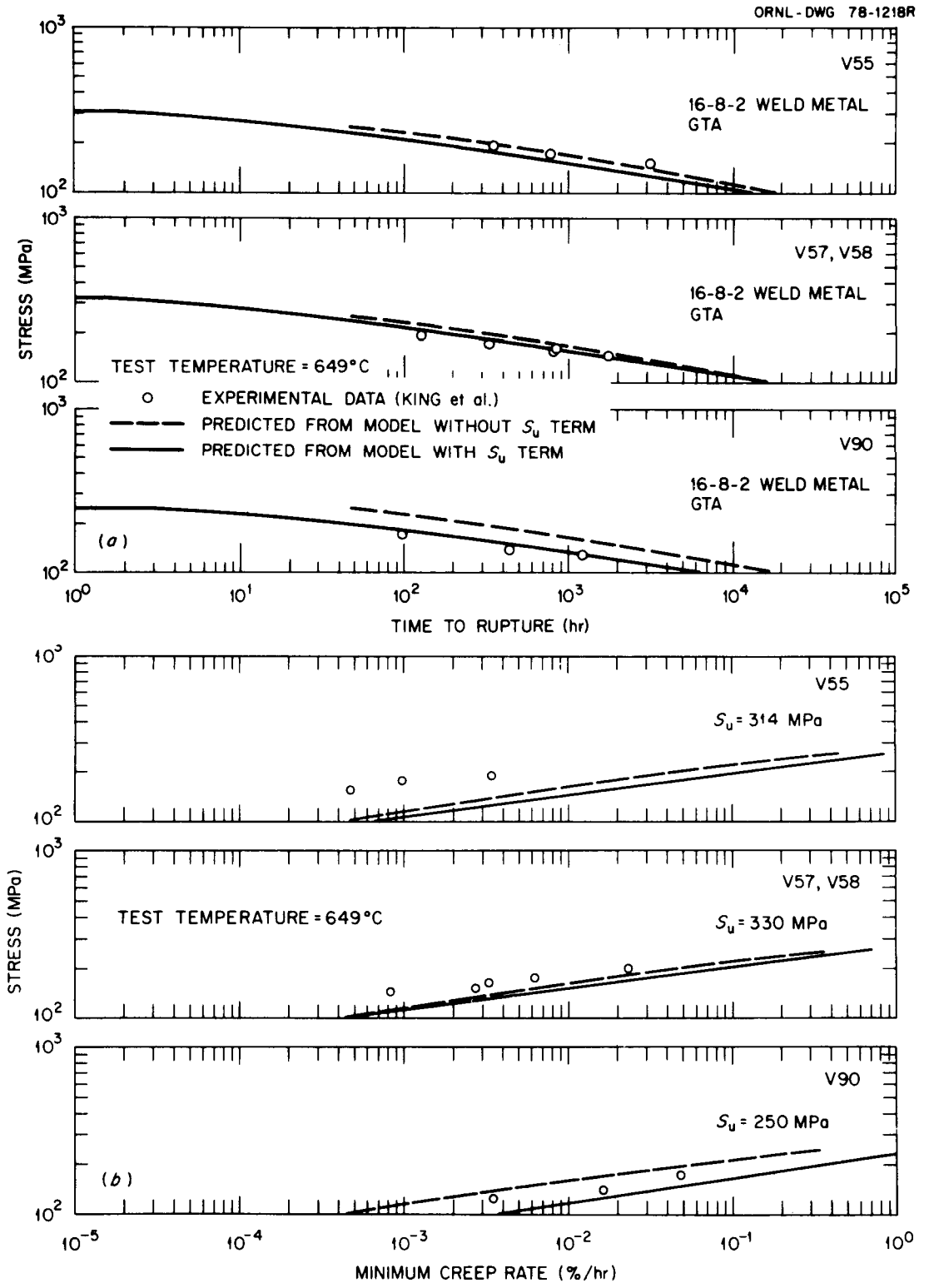

Fig. 4. Comparison of Experimental Time to Rupture and Minimum Creep Rate with Values Computed from Models with and without Elevated-Temperature S_u for GTA 16-8-2 Welds at 649°C (King et al. Data).

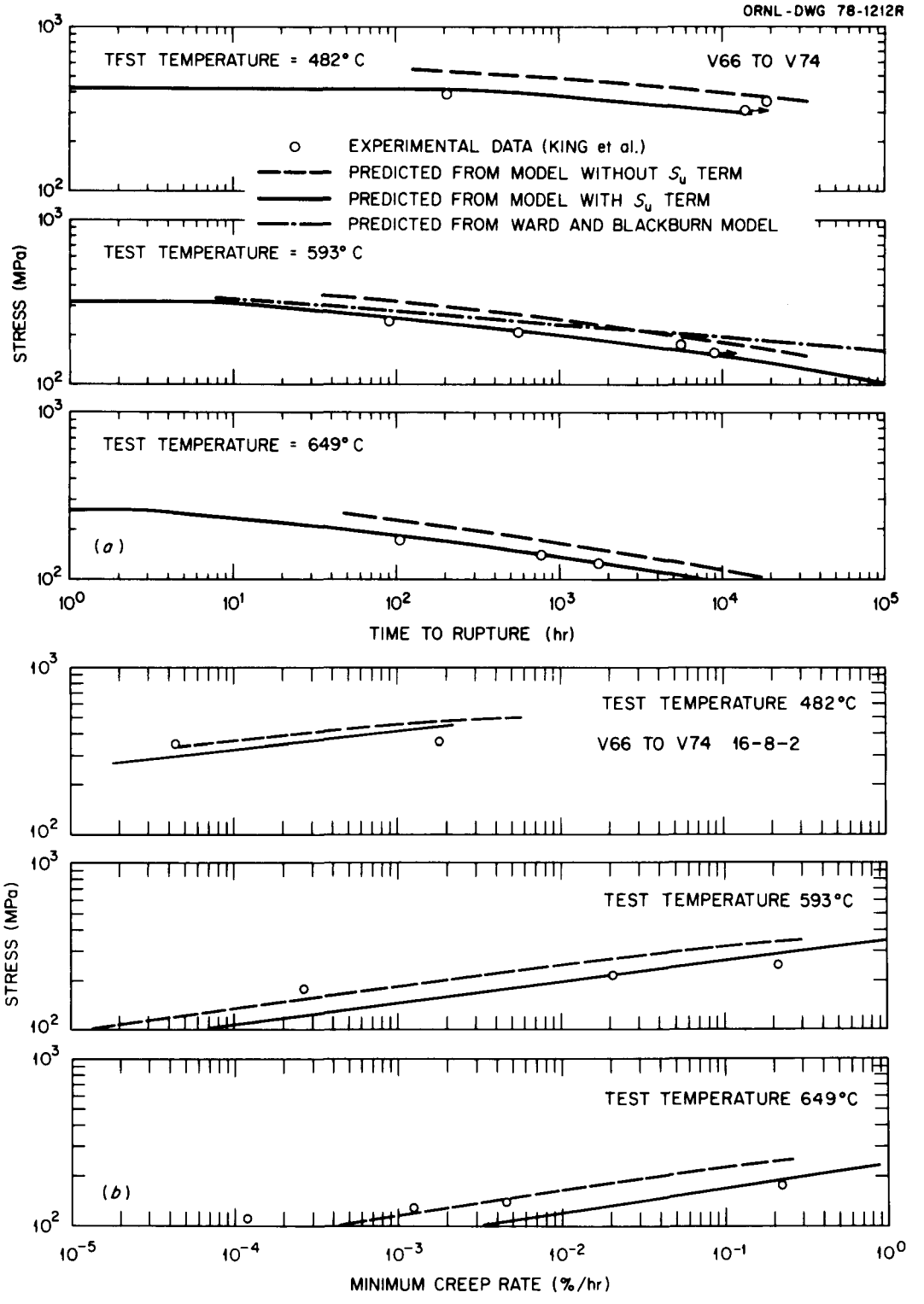

Fig. 5. Comparison of Experimental Time to Rupture and Minimum Creep Rate with Values Computed from Models with and without Elevated-Temperature S_u for GTA 16-8-2 Welds at 482, 593, and 649°C (King et al. Data).

welds showed lower rates than the average curve for the base metal. In two out of the six welds, the S_u-containing model did not help in predicting closely their creep rate behavior. Figure 5 shows that the t_r behavior of welds V-66 to V-74 can be predicted closely at all three test temperatures, 482, 593, and 649°C. The $\dot{e}_m$ predictions again do not match the data. This point will be amplified in the discussion section.

Figure 5(a) also includes the t_r values predicted from the Ward and Blackburn model.[7] It should be noted that their model, which was derived for the weld metal at a single test temperature (593°C), predicts the experimental data for welds V-66 through V-74 far more poorly than the predictions made from the base metal model in conjunction with the elevated-temperature S_u of the weld metal. Ward and Blackburn[7] made no attempt to derive a model for the minimum creep rate data.

Types 308, 316, and 16-8-2 Stainless Steel Welds (HEDL Data[8])

The welds were identified by letters A through S and were made by SA, GMA, and SMA processes. The details of weld designation and description are given in Table 1 of ref. 8. The welds were tested in either the longitudinal or the transverse direction. Some welds were tested as welded and the others postweld heat-treated. The comparisons of predicted and experimental data for various welds are shown in Figs. 6 through 15.

Figures 6(a) through 9(a) show that the t_r for almost all type 308 stainless steel welds were less than the average curves (obtained from models without S_u) for the base metal. Only the transverse composite of weld J [Fig. 8(a)] showed t_r values above the average curve for the base metal. Whether above or below the base metal average, the model containing S_u predicted the rupture behavior in close agreement with the experimental data. Figures 6(a) through 9(a) also show that S_u-based models can predict the weld metal t_r values closely for both the as-welded and the postweld heat-treated material. Figures 6(b) through 9(b) show that the S_u-based models also result in

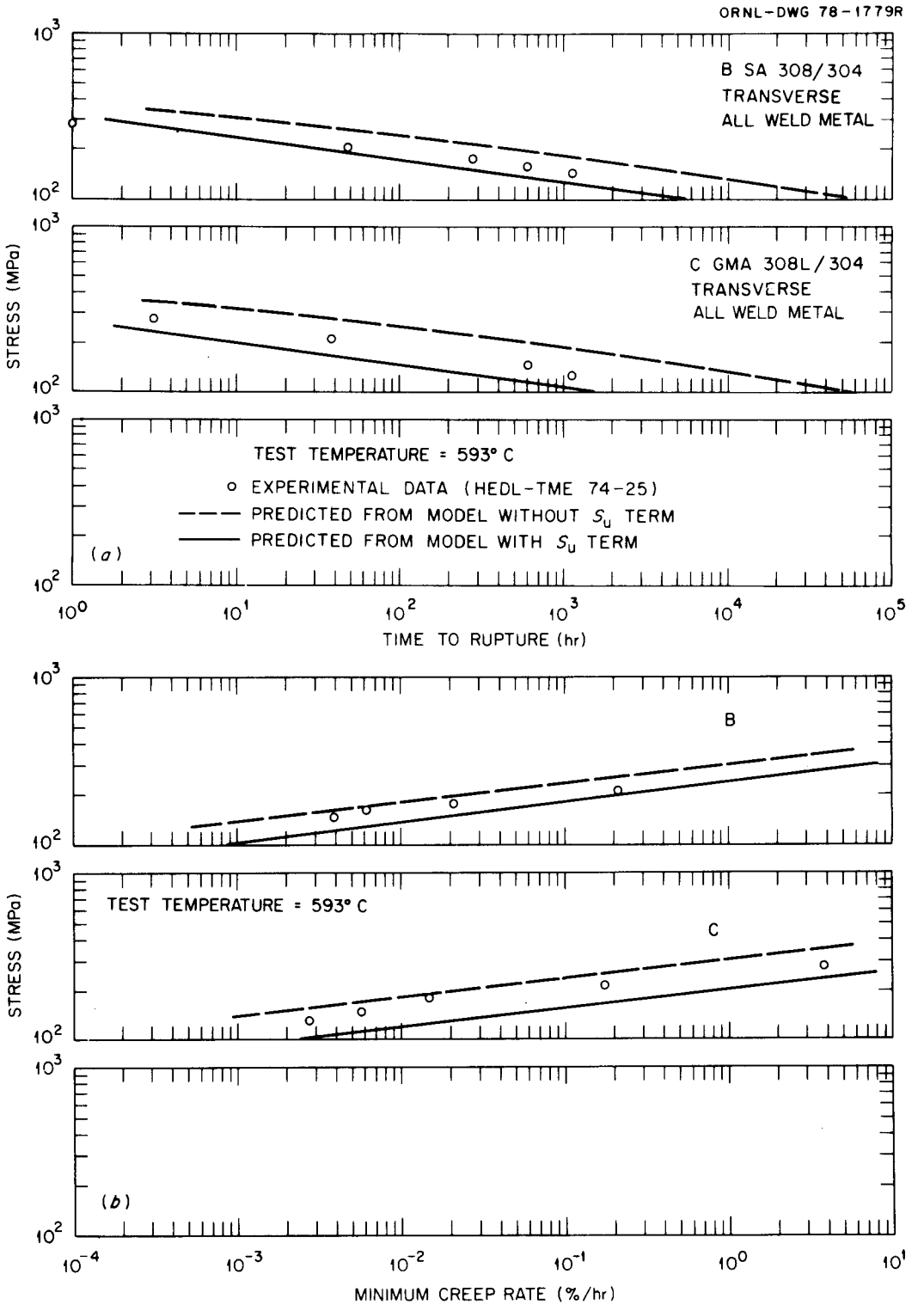

Fig. 6. Comparison of Experimental Time to Rupture and Minimum Creep Rate with Values Computed from Models with and without Elevated-Temperature S_u for two Type 308 Stainless Steel Welds at 593°C (HEDL Data).

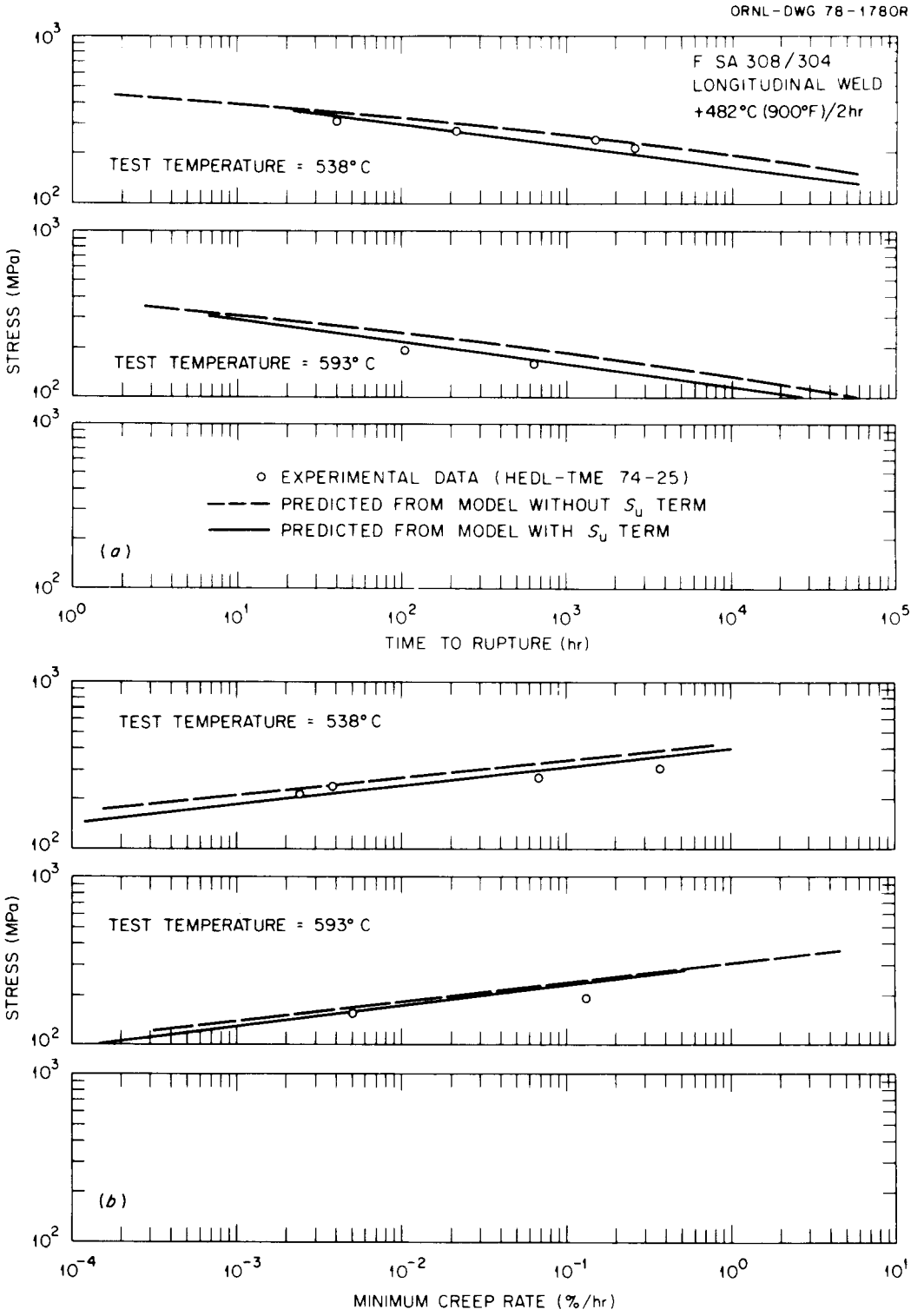

Fig. 7. Comparison of Experimental Time to Rupture and Minimum Creep Rate with Values Computed from Models with and without Elevated-Temperature S_u for a Type 308 Stainless Steel Weld at 538 and 593°C (HEDL Data).

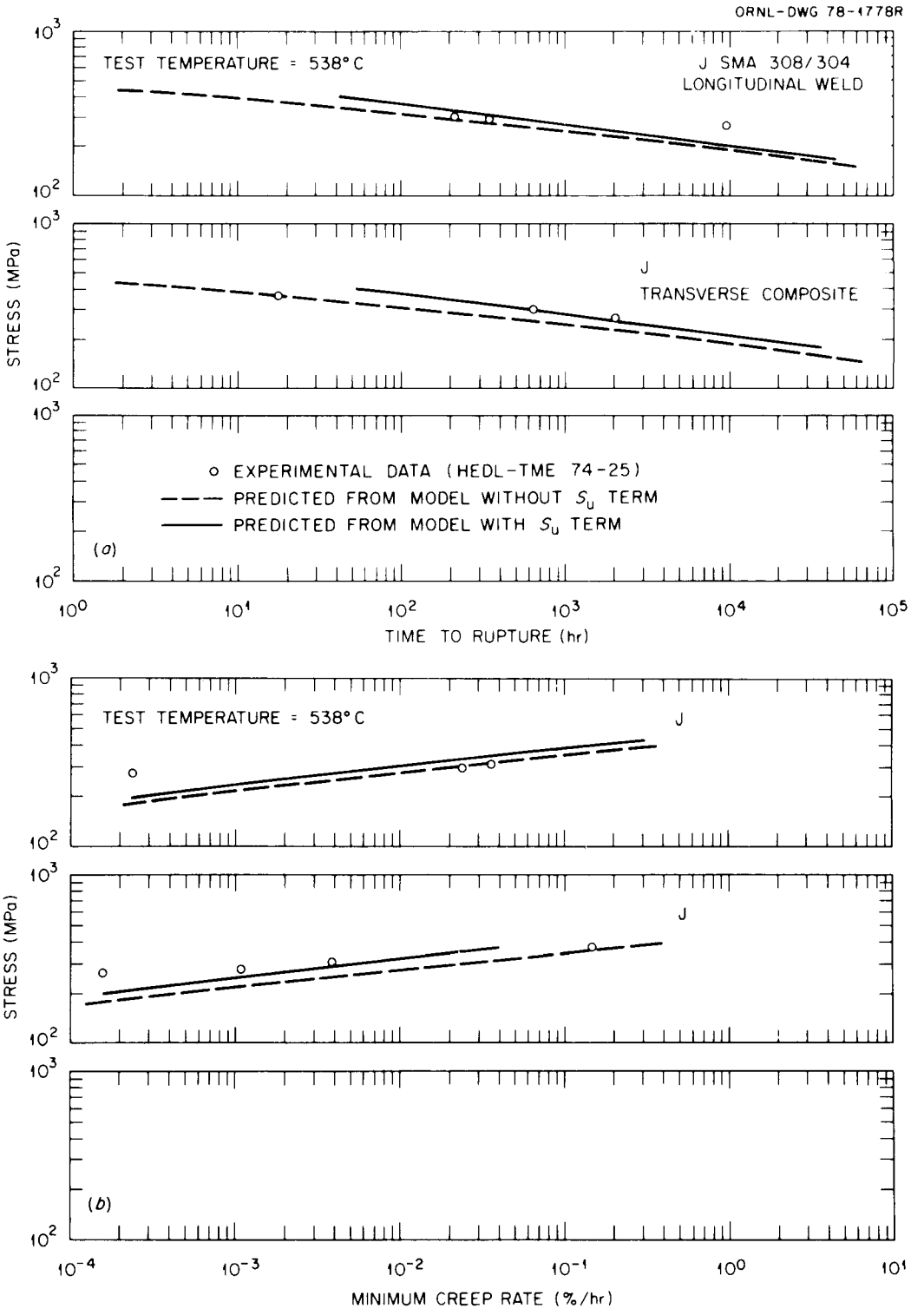

Fig. 8. Comparison of Experimental Time to Rupture and Minimum Creep Rate with Values Computed from Models with and without Elevated-Temperature S_u for a Type 308 Stainless Steel Weld and a Composite at 538°C (HEDL Data).

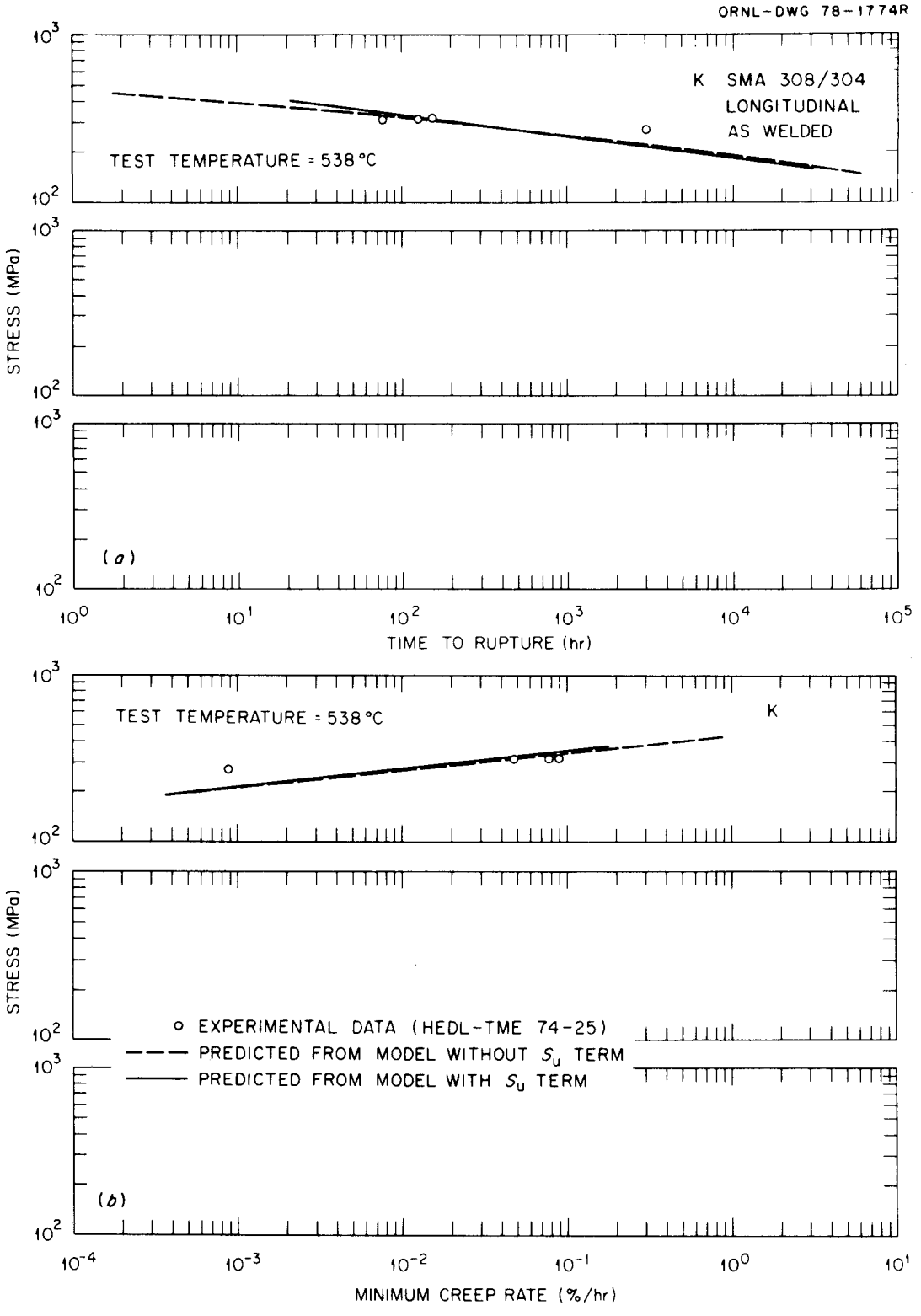

Fig. 9. Comparison of Experimental Time to Rupture and Minimum Creep Rate with Values Computed from Models with and without Elevated-Temperature S_u for a Type 308 Stainless Steel Weld at 538°C (HEDL Data).

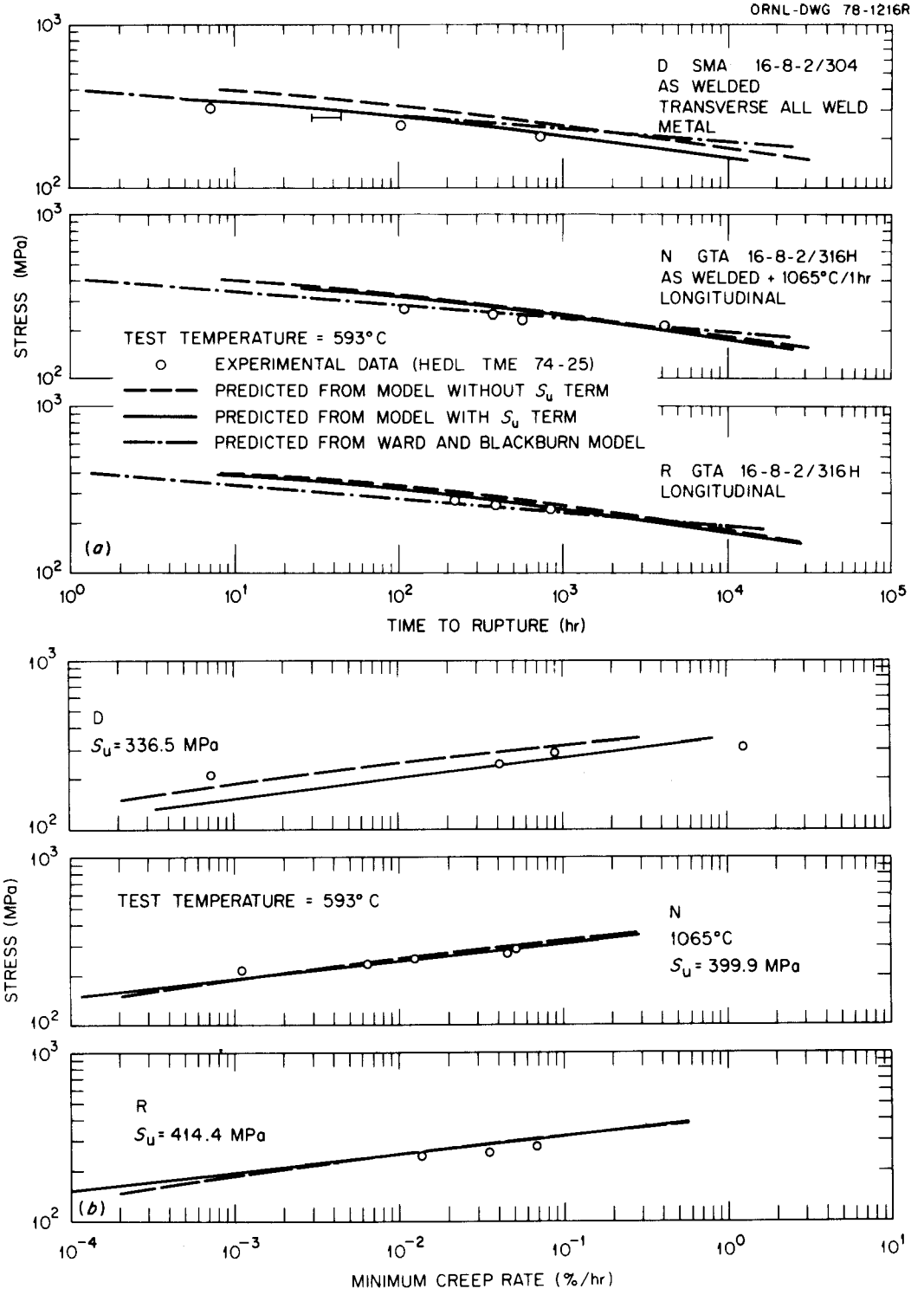

Fig. 10. Comparison of Experimental Time to Rupture and Minimum Creep Rate with Values Computed from Models with and without Elevated-Temperature S_u for Three 16-8-2 Welds at 593°C (HEDL Data). Predicted values from Ward and Blackburn models are also included in (a).

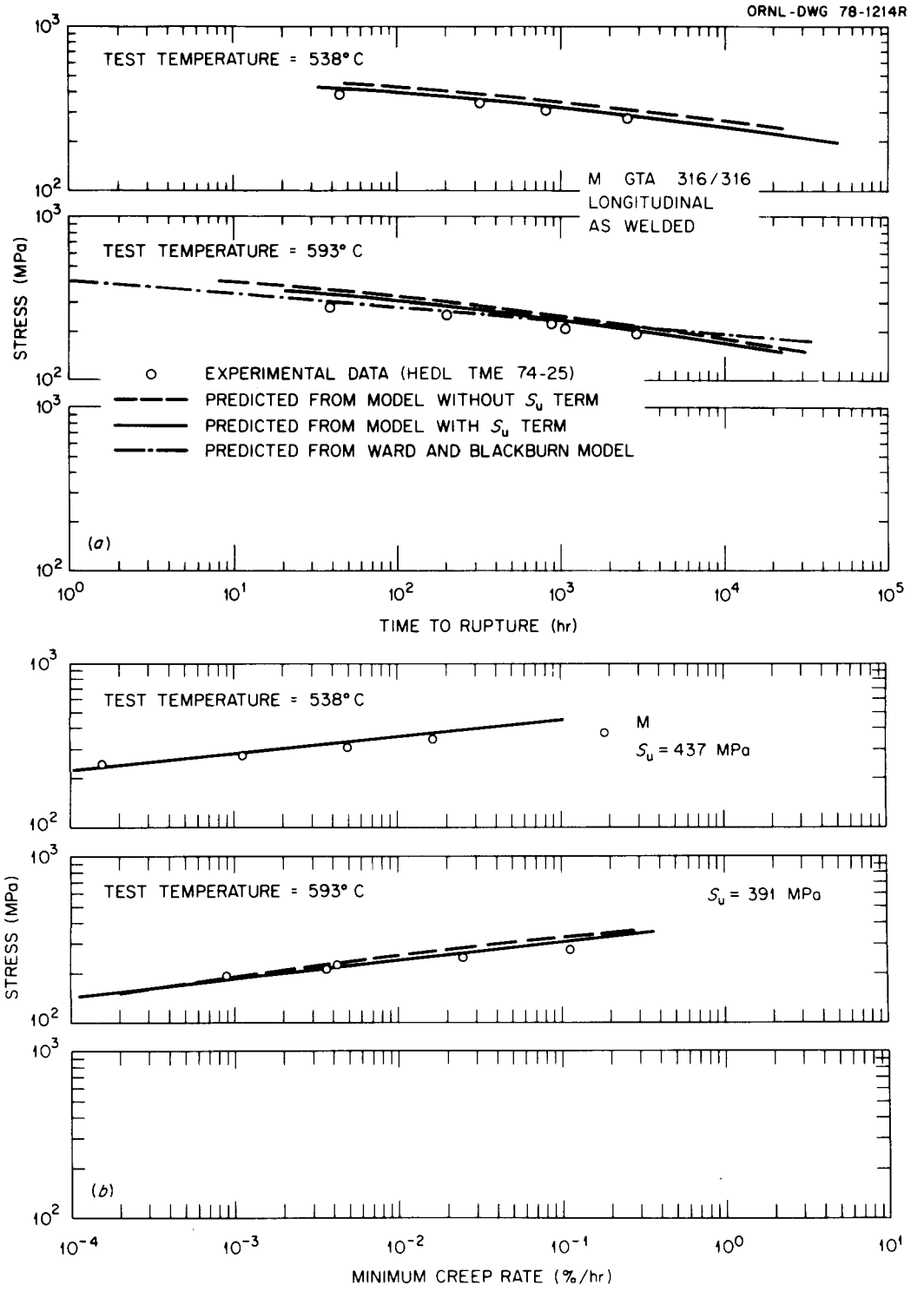

Fig. 11. Comparison of Experimental Time to Rupture and Minimum Creep Rate with Values Computed from Models with and without Elevated-Temperature S_u for a GTA Type 316 Stainless Steel Weld at 538 and 593°C (HEDL Data). Predicted values from Ward and Blackburn models are also included in (a).

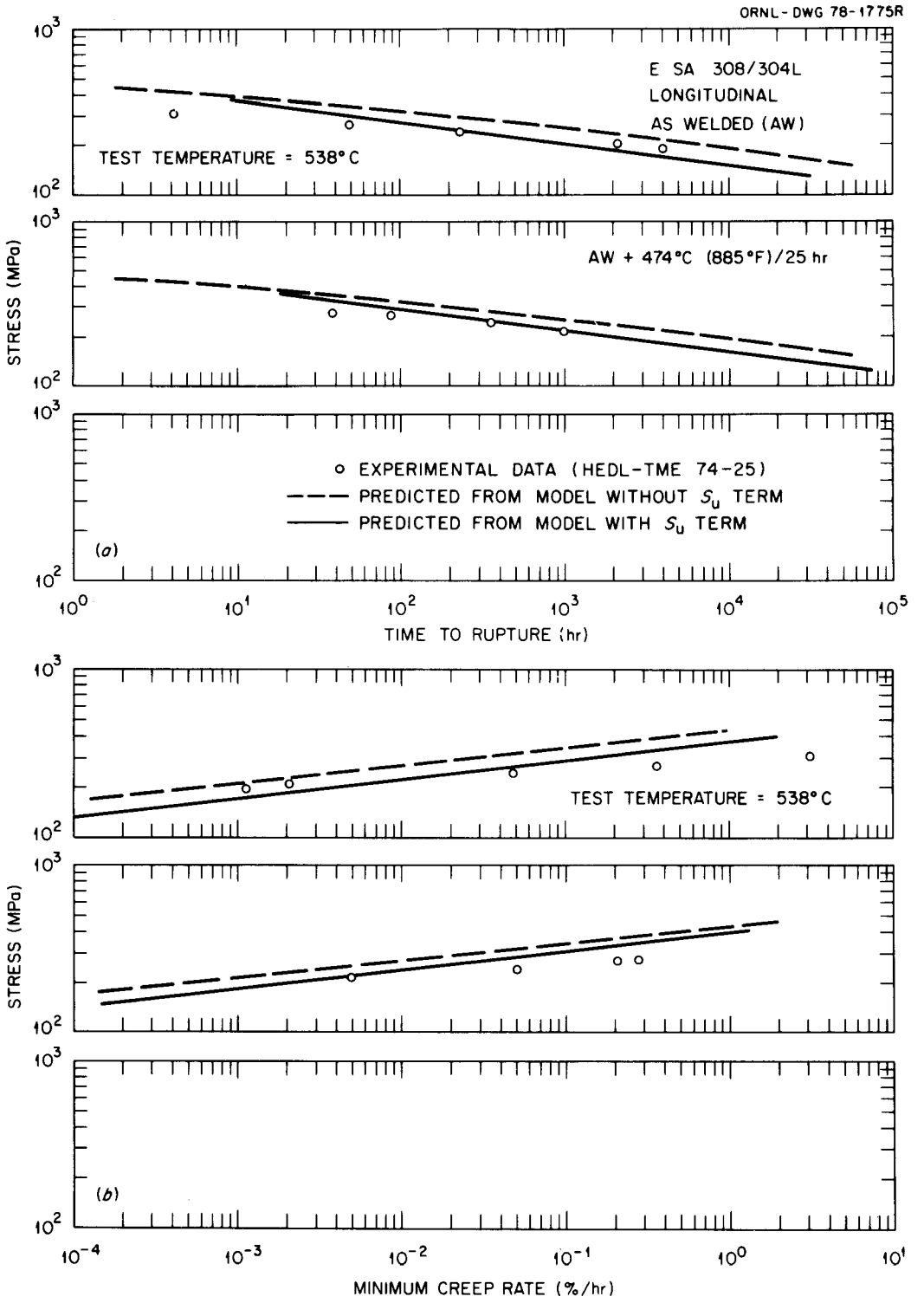

Fig. 12. Comparison of Experimental Time to Rupture and Minimum Creep Rate with Values Computed from Models with and without Elevated-Temperature S_u for a Type 308 Stainless Steel Weld at 538°C (HEDL Data). The comparisons are for material as welded or heat-treated 25 h at 474°C.

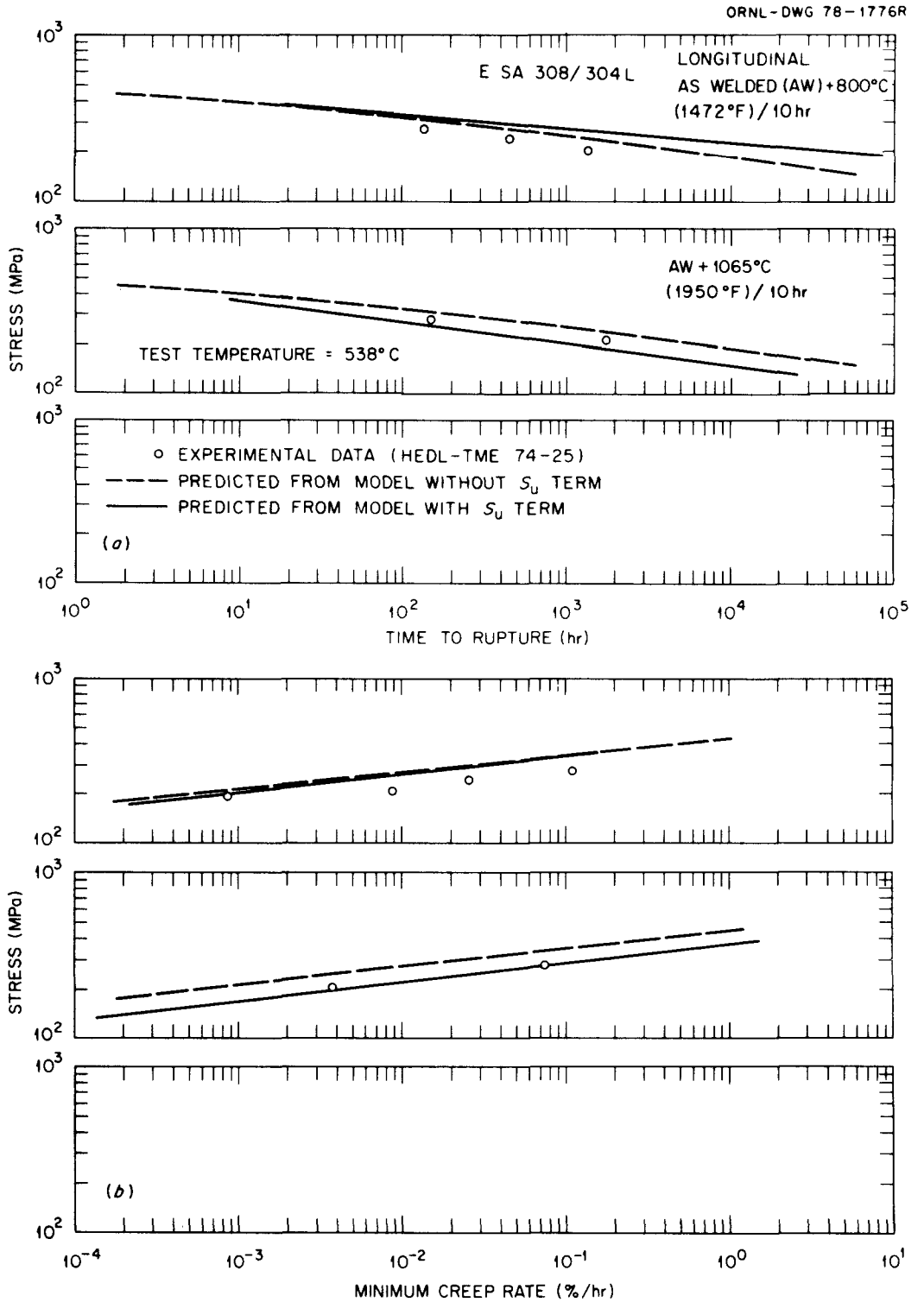

Fig. 13. Comparison of Experimental Time to Rupture and Minimum Creep Rate with Values Computed from Models with and without Elevated-Temperature S_u for a Type 308 Stainless Steel Weld at 538°C (HEDL Data). The comparisons are for the weld postweld heat-treated 10 h at 800 or 1065°C.

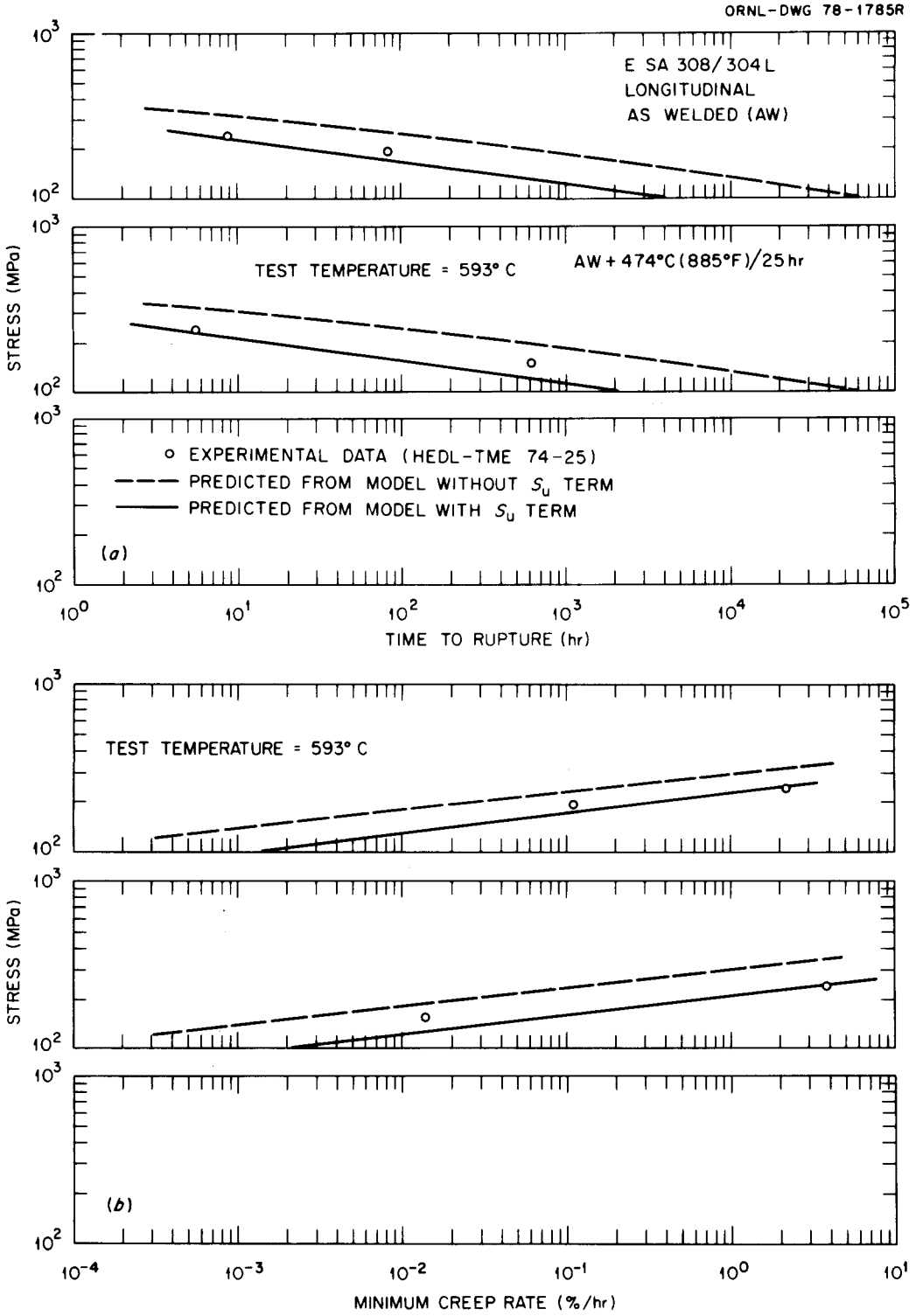

Fig. 14. Comparison of Experimental Time to Rupture and Minimum Creep Rate with Values Computed from Models with and without Elevated-Temperature S_u for a Type 308 Stainless Steel Weld at 593°C (HEDL Data). The comparisons are for material as welded or heat-treated 25 h at 474°C.

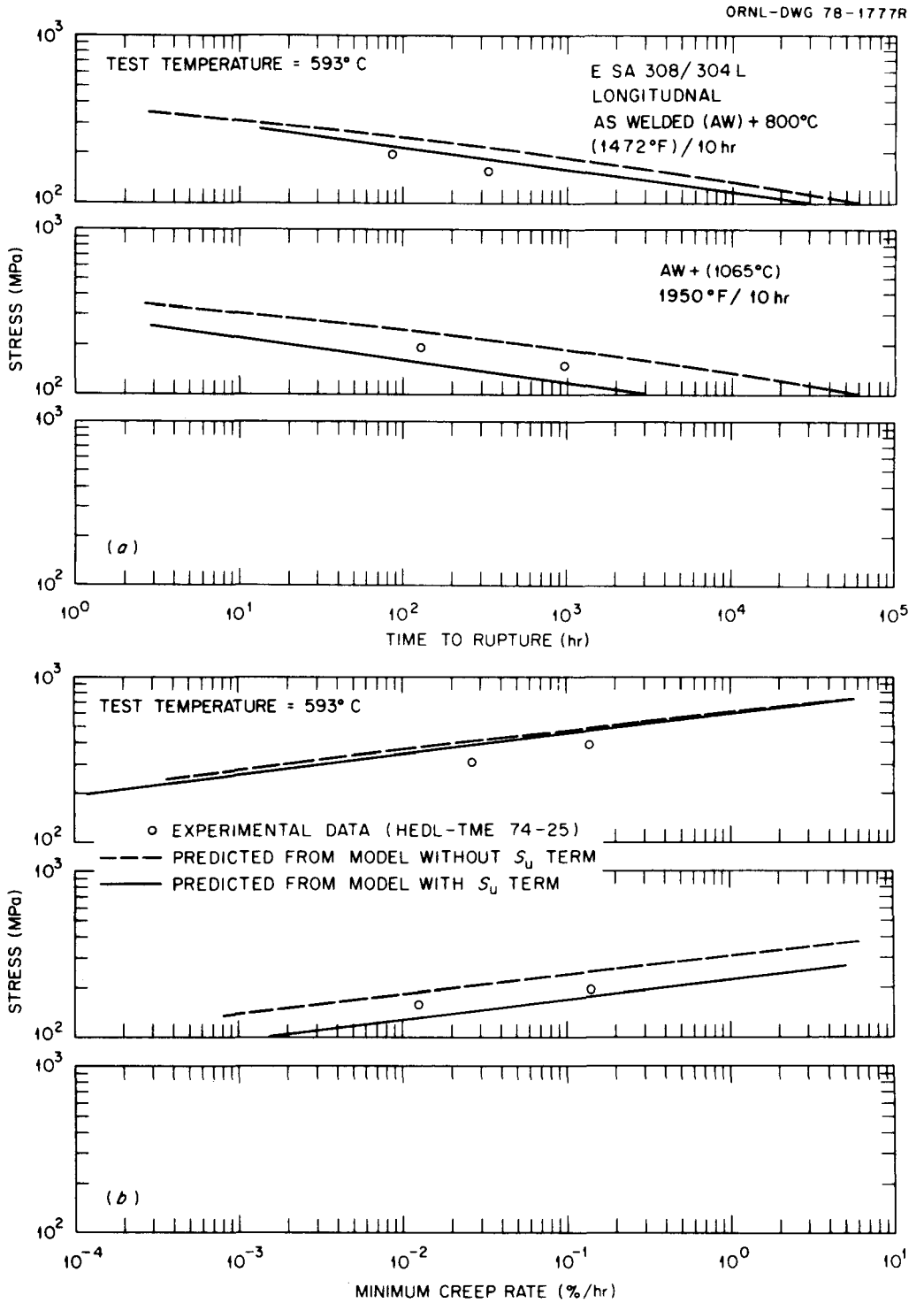

Fig. 15. Comparisons of Experimental Time to Rupture and Minimum Creep Rate with Values Computed from Models with and without Elevated-Temperature S_u for a Type 308 Stainless Steel Weld at 593°C (HEDL Data). The comparisons are for the weld postweld heat-treated for 10 h at 800 or 1065°C.

a close agreement between the predicted and the experimental $\dot{e}_m$ values for type 308 welds. This is again true for essentially all welds either as welded or postweld heat-treated.

Figures 10 and 11 compare the predicted and experimental values for the 16-8-2 and type 316 stainless steel weld metal, respectively. The weld metal t_r values are again below the average curve for the base metal. Figures 10(a) and 11(a) also show the values predicted by the Ward and Blackburn model.[7] Their model is valid only at a single test temperature, 593°C, and was derived from the data on welds made at HEDL.[8] It can be noted that the S_u-based model predicts the experimental data as well as or better than the Ward and Blackburn model.[7] Furthermore, our model can be applied at temperatures other than 593°C.

Figures 10(b) and 11(b) show that the $\dot{e}_m$ of these welds can also be predicted closely by our model containing an elevated-temperature S_u term.

When the duplex austenitic-ferritic stainless steel alloys are exposed to elevated temperatures, metallurgical instabilities associated largely with the ferrite can have deleterious effects on the mechanical properties. Thermal effects arise from postweld heat treatments and/or elevated service temperatures. Ductility losses (or embrittlement) can occur by different mechanisms in two distinct time-temperature regimes. At temperatures in the range 593 to 927°C (1100 to 1700°F), the ferrite in many alloys tends to transform to sigma phase, while at temperatures below about 540°C (1000°F) a phenomenon termed "885°F embrittlement" has been observed. A detailed literature review on both the sigma phase and "885°F embrittlement" is available in ref. 8.

Weld E of type 308 stainless steel, which contained about 12% ferrite, was subjected to various heat treatments in the as-welded condition. These treatments included 10 h at 474°C (for 885°F embrittlement), 25 h at 800°C (for sigma effects), and 10 h at 1065°C (for solution annealing effects). Creep data on material both as welded and postweld heat-treated are given in Figs. 12 through 15. The ferrite number measurements after heat treatments were not available, so the extent of transformation after the indicated heat treatments is unknown.

The thermal aging studies presented in Figs. 12 through 15 were carried out on as-welded material. Limited creep data were also obtained on material that was aged 10 h at 800°C after prior solution annealing for 1 h at 1065°C (Figs. 16 and 17). Once again the lack of ferrite measurement after heat treatment obscures the extent of ferrite to sigma transformation. From the ongoing program on ferrite transformation at ORNL, we expect that 10 h at 800°C will nearly transform all ferrite to sigma phase (or, more positively, a nonmagnetic phase).

Figures 12(a) through 17(a) show that at both test temperatures, 538 and 593°C, the S_u-based models predict the experimental rupture life data closely for all heat treatments except the one in which sigma heat treatment was introduced without prior postweld heat treatment. For such a heat treatment the S_u-based model predicted too long t_r values. The same observation was true for the $\dot{e}_m$ data after various heat treatments, Figs. 12(b) through 17(b).

We will show later that the t_r and $\dot{e}_m$ data were predicted correctly, when sigma phase heat treatment was given to type 316 stainless steel cast-and-worked pipe that had a starting ferrite content of about 10 FN. Similarly we will show that the creep-rupture behavior can still be predicted for castings in which sigma is formed (from δ-ferrite) during the creep test. Data in Figs. 16 and 17 have already shown that the creep-rupture behavior of type 308 stainless steel weld E is predictable when the sigma phase is produced after solution heat treatment. We therefore conclude that the poor performance of current models in predicting the rupture behavior of weld E when it was sigma heat-treated in the as-welded condition is probably a consequence of unusually high values of ultimate tensile strength reported for this material condition. Thus, we recommend additional testing on type 308 welds in the above heat-treated condition to verify the reported ultimate tensile strength values.

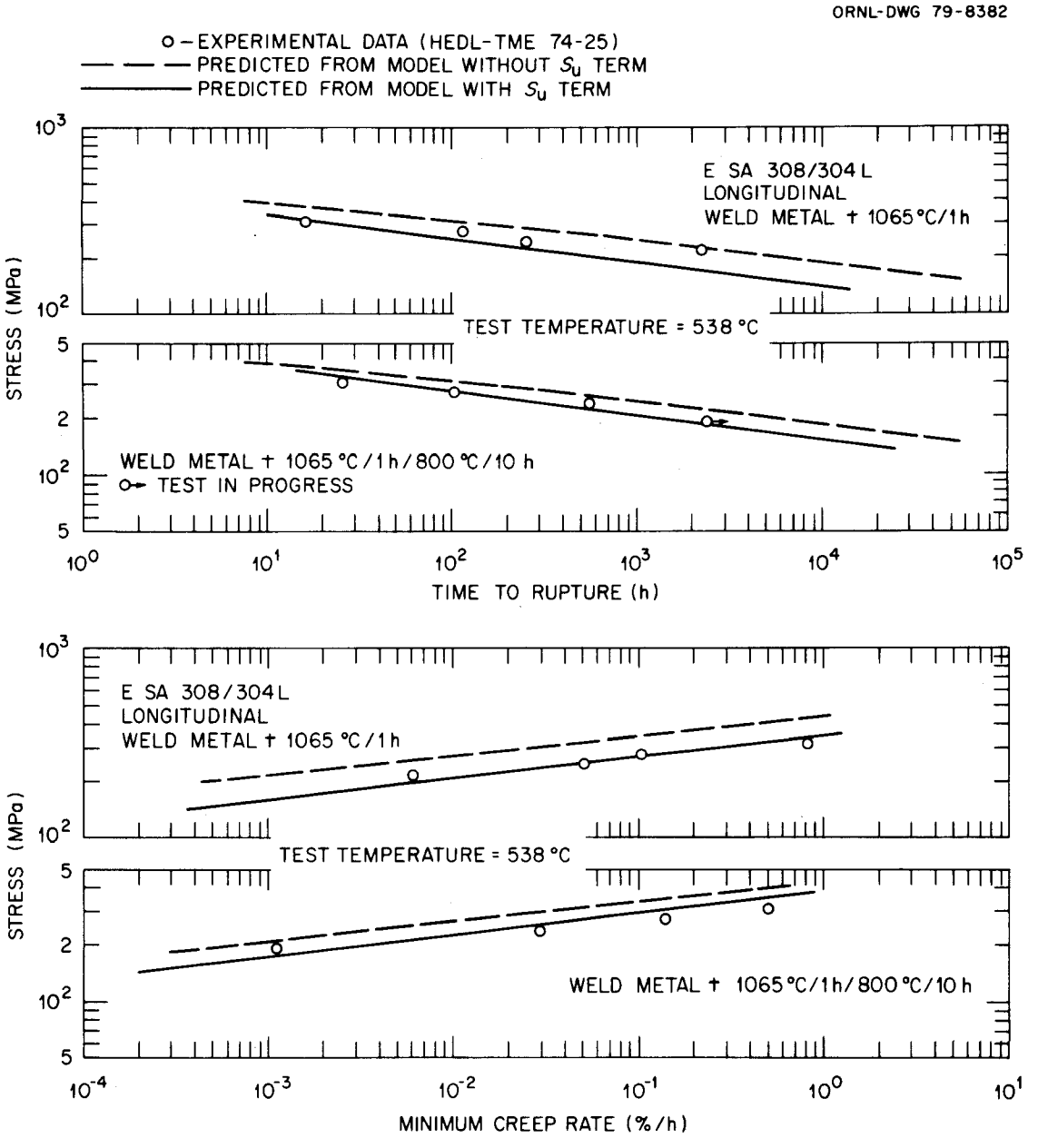

Fig. 16. Comparison of Experimental Time to Rupture and Minimum Creep Rate with Values Computed from Models with and without Elevated-Temperature S_u for a Type 308 Stainless Steel Weld at 538°C (HEDL Data). The comparisons are for the weld postweld heat-treated 1 h at 1065°C and 1 h at 1065°C plus 10 h at 800°C.

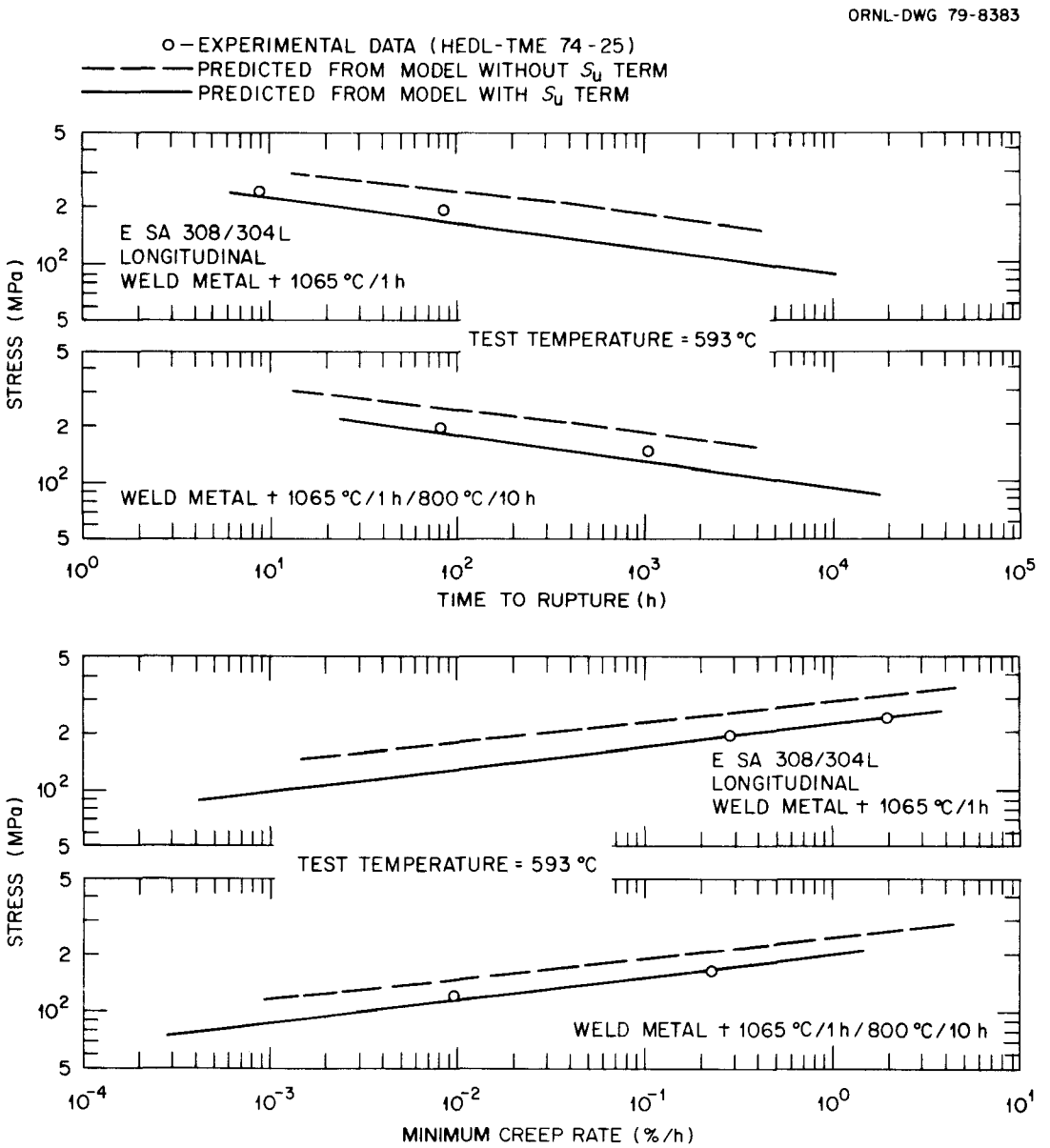

Fig. 17. Comparison of Experimental Time to Rupture and Mininum Creep Rate with Values Computed from Models with and without Elevated-Temperature S_u for a Type 308 Stainless Steel Weld at 593°C (HEDL Data). The comparisons are for the weld postweld heat-treated 1 h at 1065°C and 1 h at 1065°C plus 10 h at 800°C.

Weld-Overlaid Type 304 Stainless Steel Forging (Klueh and Canonico Data[9,10])

The intermediate heat exchanger (IHX) tubesheet of the Fast-Flux Test Facility (FFTF) is an air-melted type 304 stainless steel forging overlaid with type 308 stainless steel weld metal. To make the tube-to-tubesheet joint, the tube is butted against a prolongation machined from type 308 stainless steel filler metal and an internal bore weld is made. The overlay provides sound metal (free of nonmetallic inclusions) from which the prolongation of the tubesheet can be machined. A schematic illustration of the joint is available in refs. 9 and 10.

The weld-overlaid forging was made as follows:

An air-melted type 304 stainless steel forging with a work history similar to that of the tubesheet used by Foster-Wheeler Corporation in the FFTF was purchased from the National Forge Company. This forging was a 0.75-m-diam round that was overlaid by Foster-Wheeler Corporation by the same procedure used in the preparation of the IHX tubesheet of FFTF. Before being overlaid, the surface of the forging was machined and dye-penetrant inspected. The overlay of type 308 stainless steel filler metal was deposited by the submerged-arc welding process, using a 1.6-mm-diam wire. Six passes were made to give a weld metal buildup of about 19 mm; after overlaying, the surface was machined.

Tensile and creep data are available[9,10] from all sections: overlay, forging just below the interface, and forging at a distance from the interface. These sections were tested in both radial and tangential orientations. In addition, axial specimens were tested from the underlying forging (unaffected by the overlay process) and from across the fusion line so that the gage length contained both weld metal and forging (plus the interface).

Creep data (482, 538, and 649°C) from various sections of the overlay are compared with the predicted value curves in Figs. 18 through 21. Time to rupture for the forging and adjacent to the fusion line was significantly higher than the average values predicted for the base metal at all three test temperatures. Time to rupture for the weld

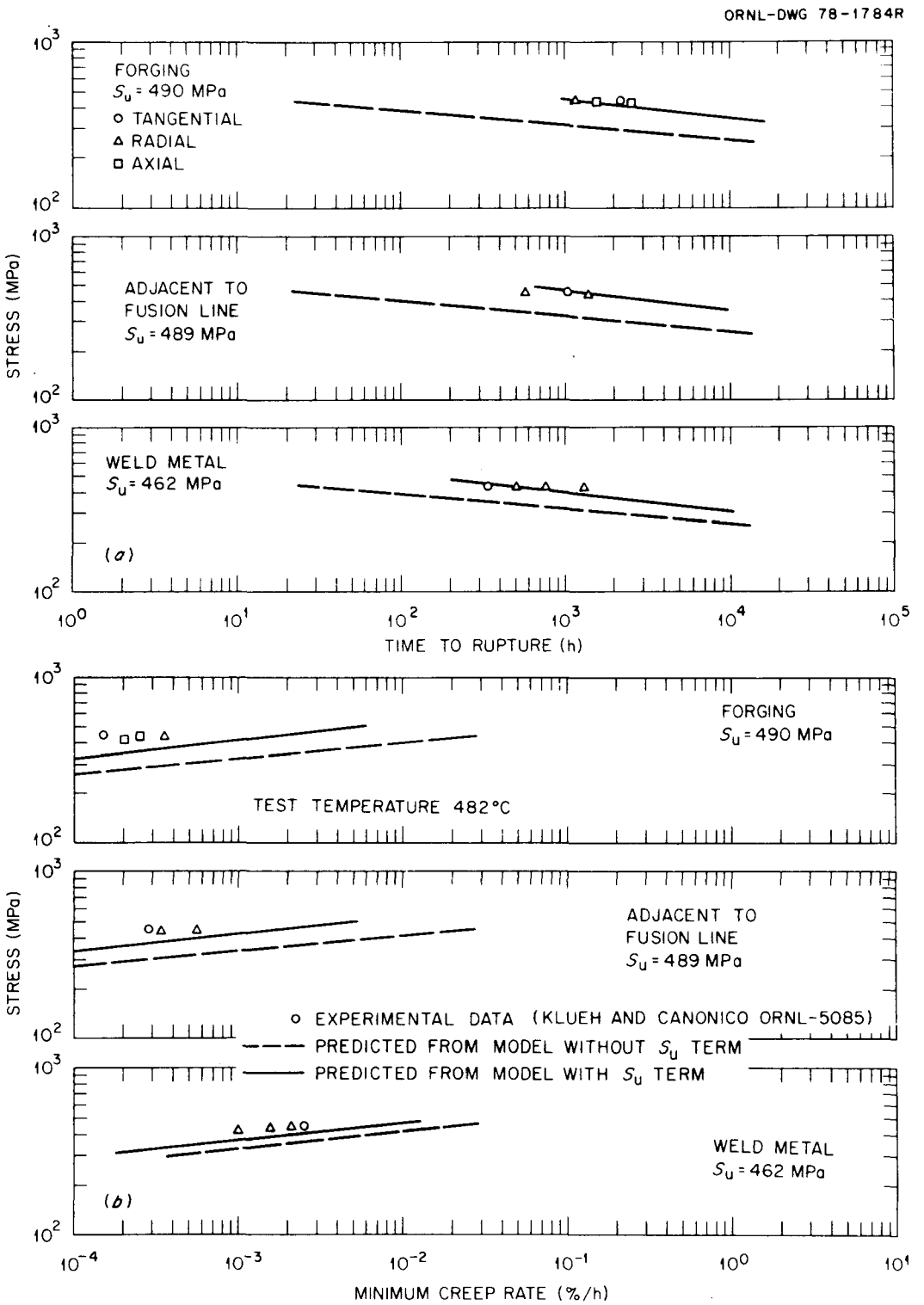

Fig. 18. Comparison of Experimental Time to Rupture and Minimum Creep Rate with Values Computed from Models with and without Elevated-Temperature S_u for Various Section of a Weld-Overlaid Type 304 Stainless Steel at 482°C (Klueh and Canonico Data).

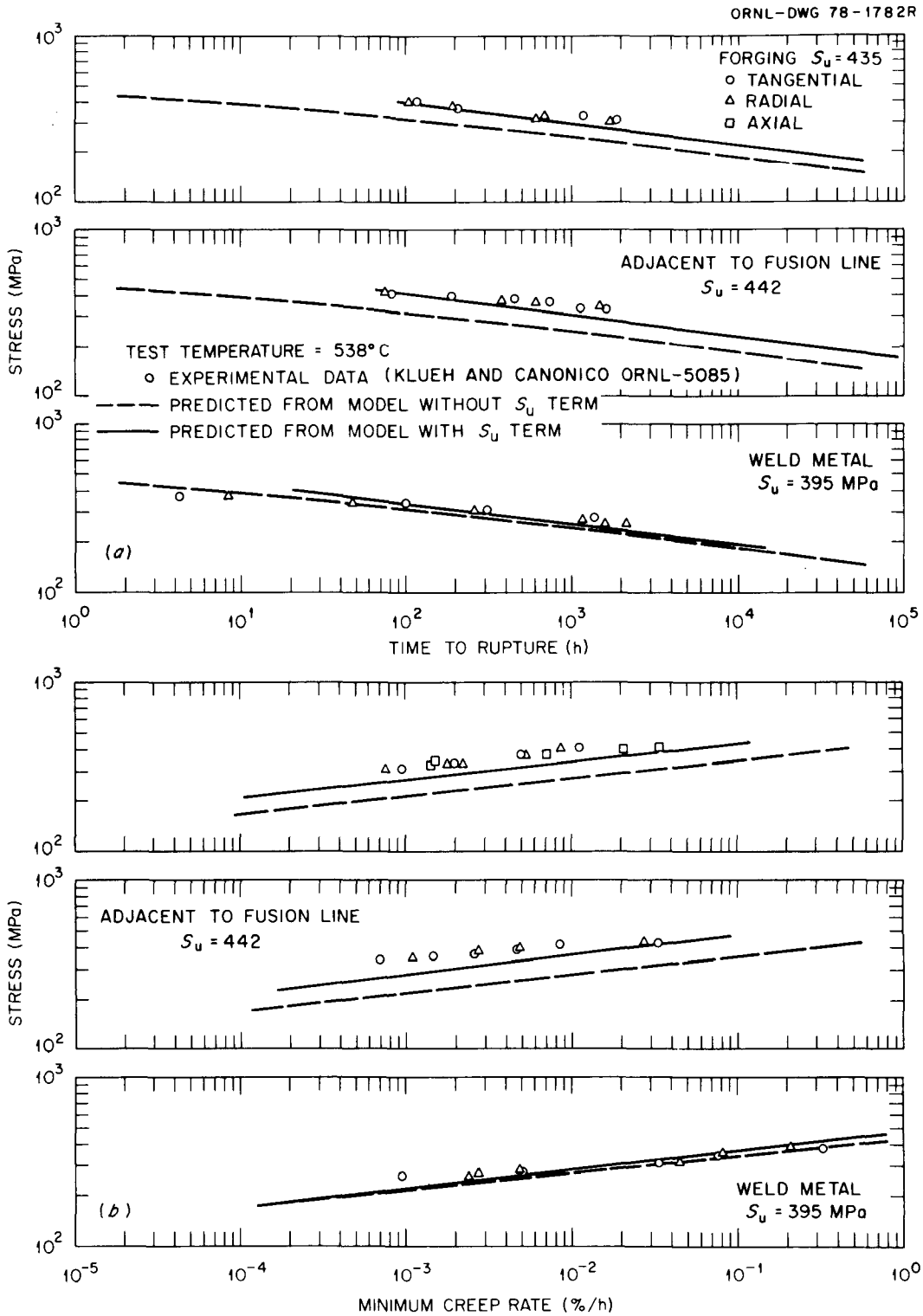

Fig. 19. Comparison of Experimental Time to Rupture and Minimum Creep Rate with Values Computed from Models with and without Elevated-Temperature S_u for Various Sections of a Weld-Overlaid Type 304 Stainless Steel at 538°C (Klueh and Canonico Data).

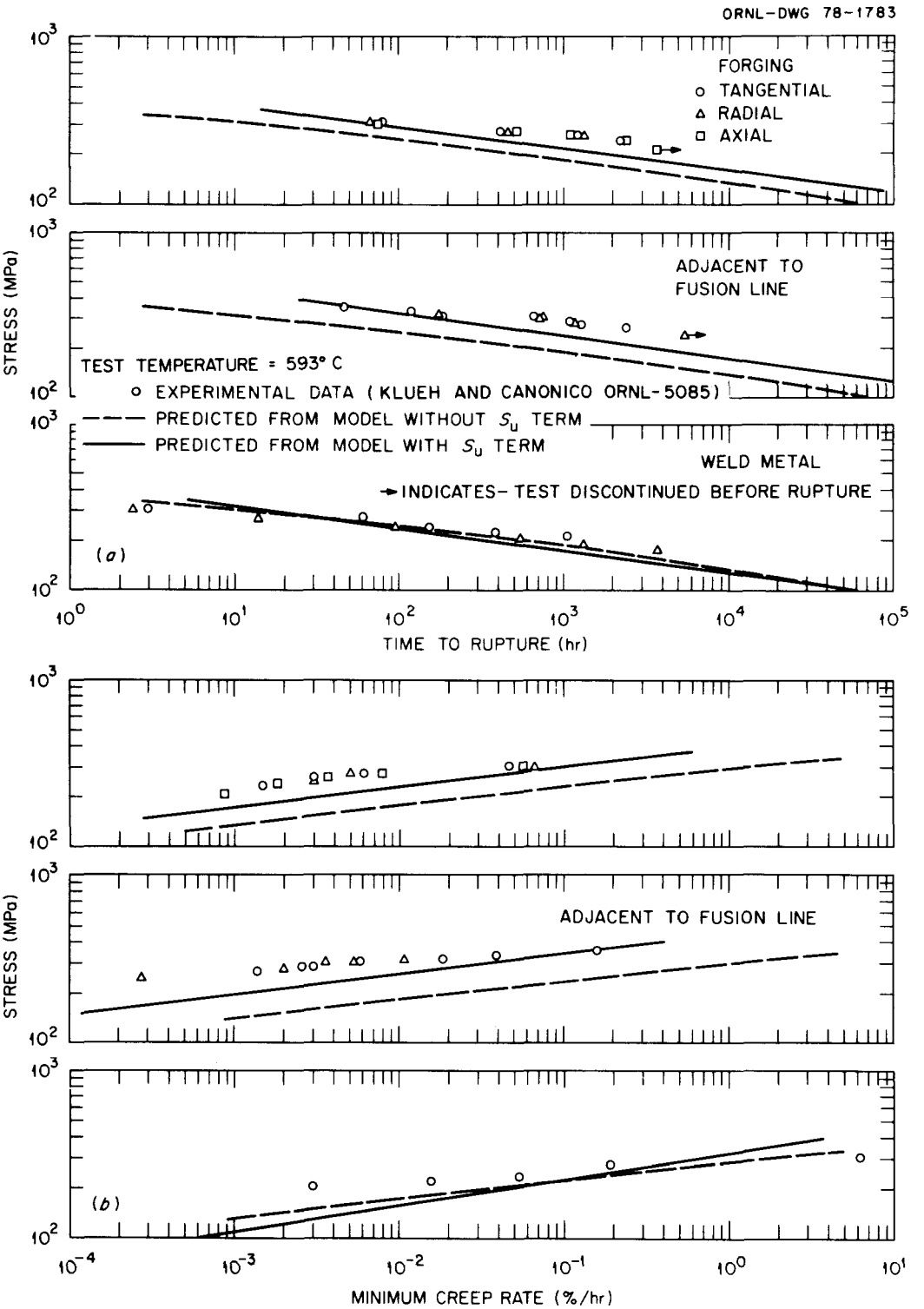

Fig. 20. Comparison of Experimental Time to Rupture and Minimum Creep Rate with Values Computed from Models with and without Elevated-Temperature S_u for Various Sections of a Weld-Overlaid Type 304 Stainless Steel at 593°C (Klueh and Canonico Data).

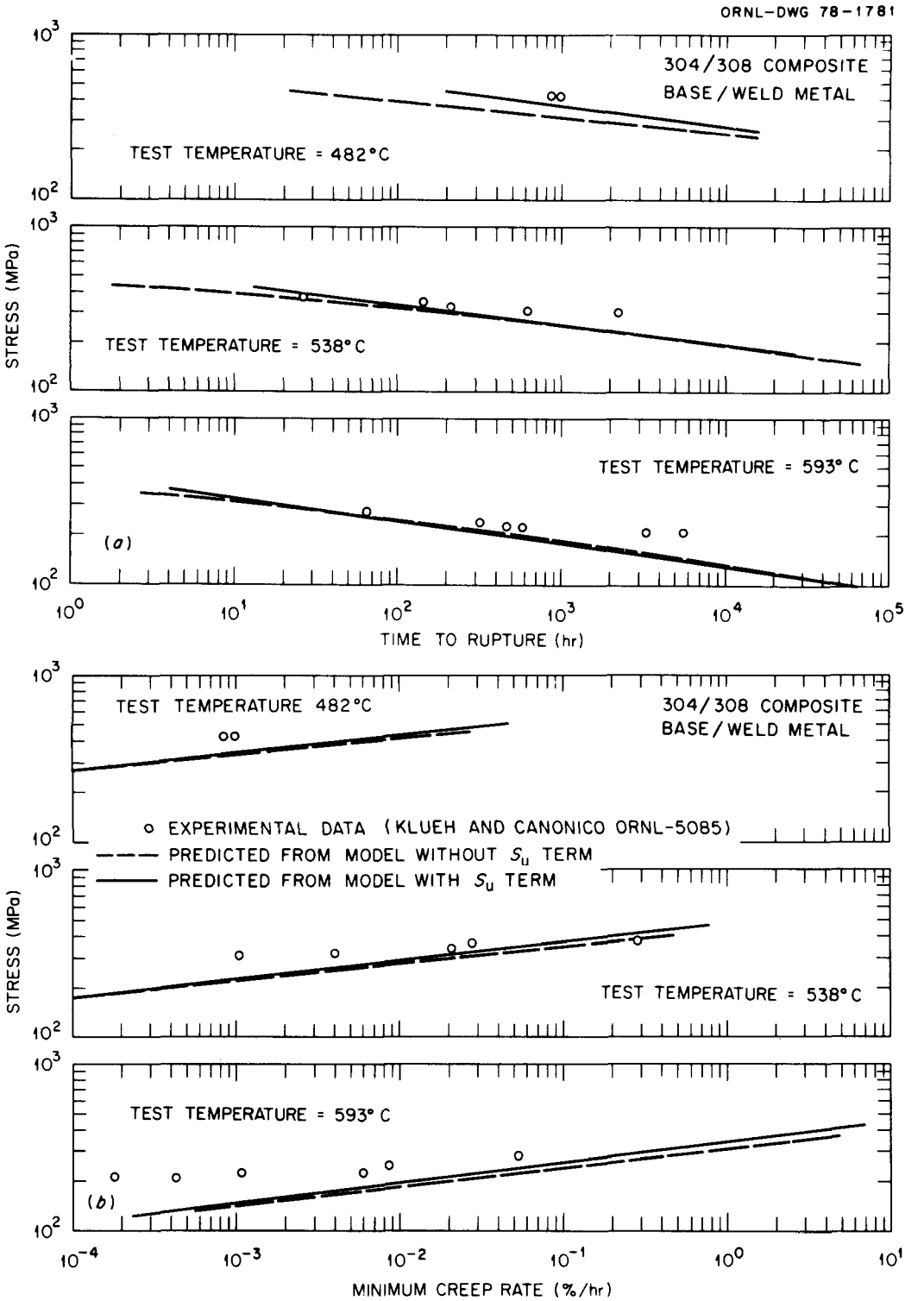

Fig. 21. Comparison of Experimental Time to Rupture and Minimum Creep Rate with Values Computed from Models with and without Elevated-Temperature S_u for Base and Weld Metal Composite Section of a Weld-Overlaid Type 304 Stainless Steel at 482, 538, and 593°C (Klueh and Canonico Data).

metal was above the base metal average only at 482°C. At higher temperatures (538 and 593°C), weld metal data coincided with the base metal average curve. The base and weld metal composite behaved similarly to the weld metal. Irrespective of whether a section was stronger than or as strong as the base metal average, the S_u-based model predicted its time to rupture closely.

For the $\dot{e}_m$ data the S_u-based models always tended to predict the divergence from average behavior in the right direction. However, there were still some differences between the data and the predicted value curves. It should be noted that S_u-based models provide predicted values at least a factor of 10 closer to the experimental data than the average values predicted from a model without S_u. This is true for data on all sections and at all three test temperatures, 482, 538, and 593°C.

Weld Metal Data on Formed-and-Welded Pipes (McEnerney and Sikka[11,12] Data)

McEnerney and Sikka[11,12] have recently collected tensile and creep data on welds in five formed-and-welded pipes. The pipe identification, fabrication procedure, filler wire addition, welding process, and postweld heat treatment are summarized in Table 1. Note that all pipes were given a postweld solution heat treatment. Axial and circumferential specimens were tensile tested for the base metal region, whereas longitudinal and transverse specimens were tensile and creep tested from the weld metal region. The longitudinal specimens were expected to contain all weld metal. However, because of the weld configuration some longitudinal specimens were mostly weld metal with only a small portion base metal. The transverse specimen was a composite and contained weld metal in the center and base metal on either side. Tensile and creep data on these pipe welds are available in other reports.[11,12]

Table 1. Summary of Identification, Fabricator, Welding Process, Filler Metal, and Final Heat Treatment for Formed-and-Welded 0.91-mm-OD by 13-mm-Wall Pipes of Type 316 Stainless Steel

Identification	Fabricator	Welding Process	Filler Metal	Final Heat Treatment[a]	
				Temperature (°C)	Time (h)
E-13	Youngstown Welding and Engineering Company	GTA with both hot and cold wire additions	16-8-2	1060	0.5
F-14	Trent Tube Division of Crucible Steel Company of America	GTA with cold wire addition	16-8-2	1066	0.2 (minimum)
G-15	Swepco Tube Corporation	GTA with cold wire addition and SA	316	1093	0.5
G-16	Swepco Tube Corporation	Autogeneous GTA	None	1038–1066	0.5
H-22	National Annealing Box Company	SA	16-8-2	1066	0.75

[a]Followed by water quench.

Figures 22 through 26 compare experimental data with the predicted curves for t_r and $\dot{e}_m$. The elevated-temperature ultimate tensile strengths for the longitudinal and transverse specimens were not significantly different, so the predicted curves are based on the average values for the two types of specimens. These figures show good agreement between the predicted curves and the experimental rupture data on all welds. However, the minimum creep rate data showed good agreement only for E-13, F-14, and H-22 welds. The experimental values for G-15 and G-16 welds were more than an order of magnitude lower than the predicted values. This observation is similar to that made for King et al.[6] data on several 16-8-2 welds [Figs. 3(b)–5(b)]. The poor agreement for the minimum creep rate occurs as a consequence of flat-top creep curves often observed for the weld metal, Fig. 27. The extent of flatness differs from weld to weld. Current models cannot predict the minimum creep rate unless the creep curves are classical. Reasons for such flat-top creep curves are not currently known. However, systematic work in this area is planned in the near future to understand these reasons. A thorough classification of creep curve type for various welds will also be conducted, so that the minimum creep rate models may be modified if so desired.

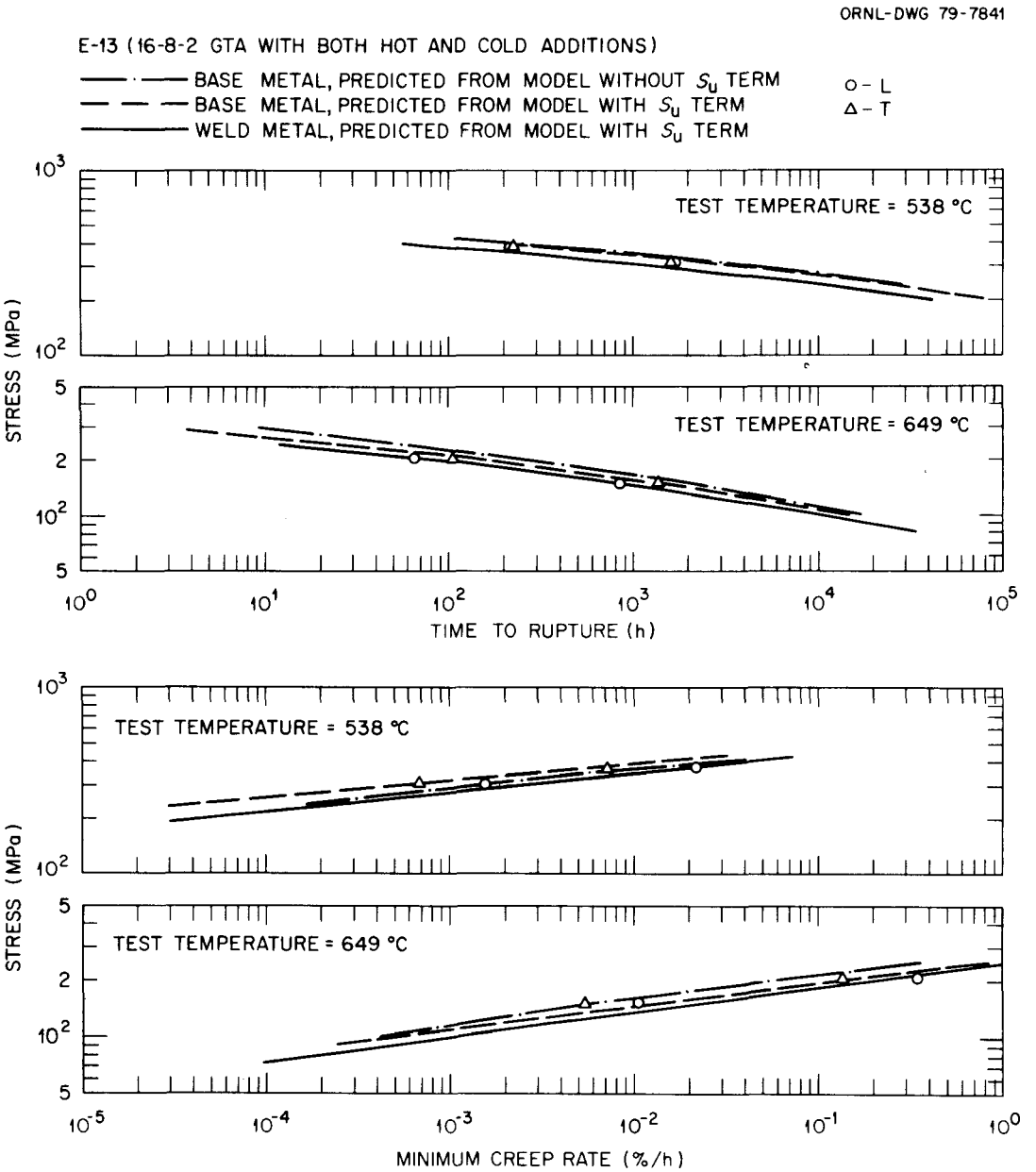

Fig. 22. Comparison of Experimental Time to Rupture and Minimum Creep Rate with Values Computed from Models with and without Elevated-Temperature S_u for 16-8-2 GTA Weld Metal and the Weldment Specimens Removed from Formed-and-Welded Pipe E-13 of Type 316 Stainless Steel (McEnerney and Sikka Data).

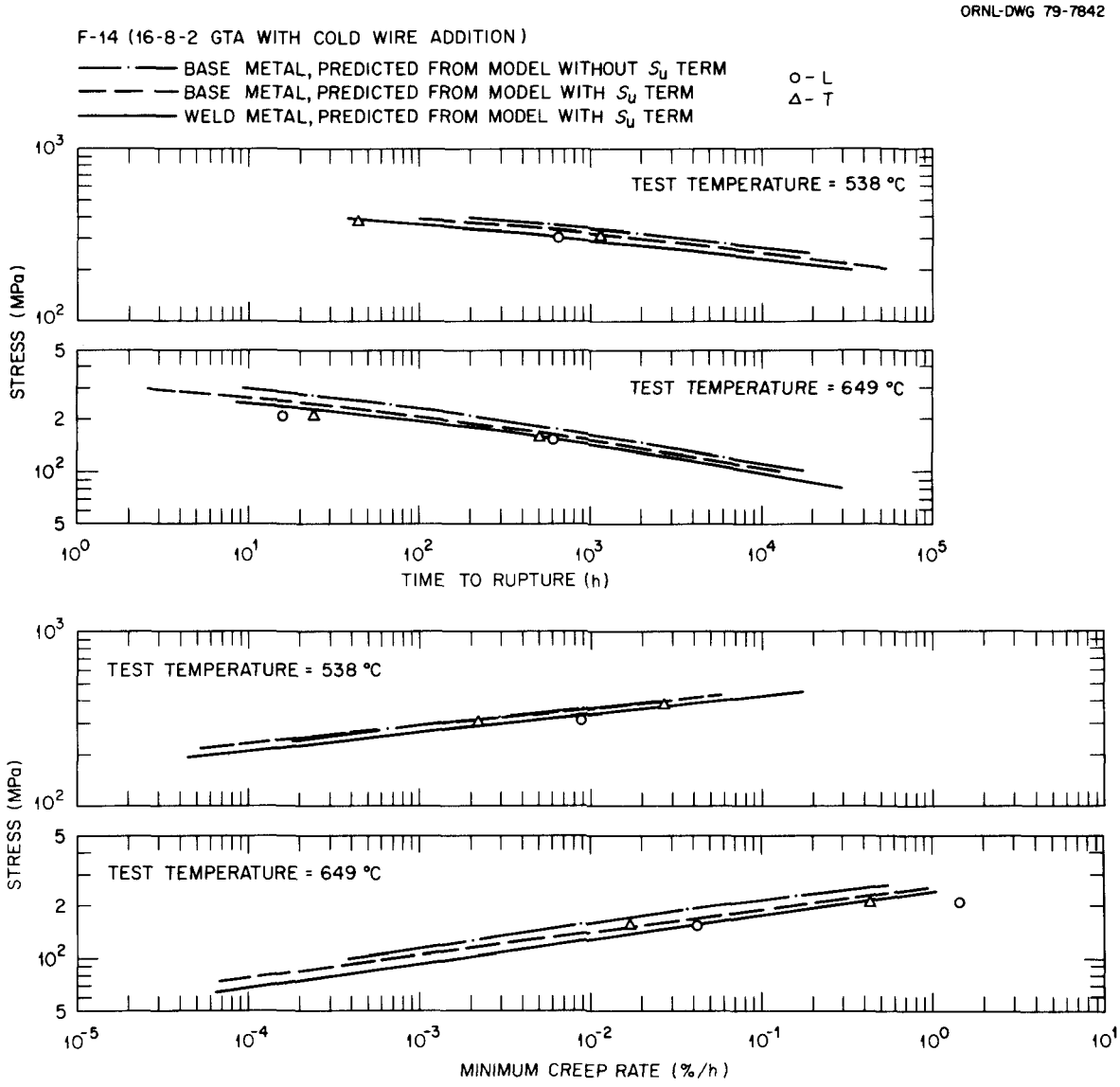

Fig. 23. Comparison of Experimental Time to Rupture and Minimum Creep Rate with Values Computed from Models with and without Elevated-Temperature S_u for 16-8-2 GTA Weld Metal and the Weldment Specimens Removed from Formed-and-Welded Pipe F-14 of Type 316 Stainless Steel (McEnerney and Sikka Data).

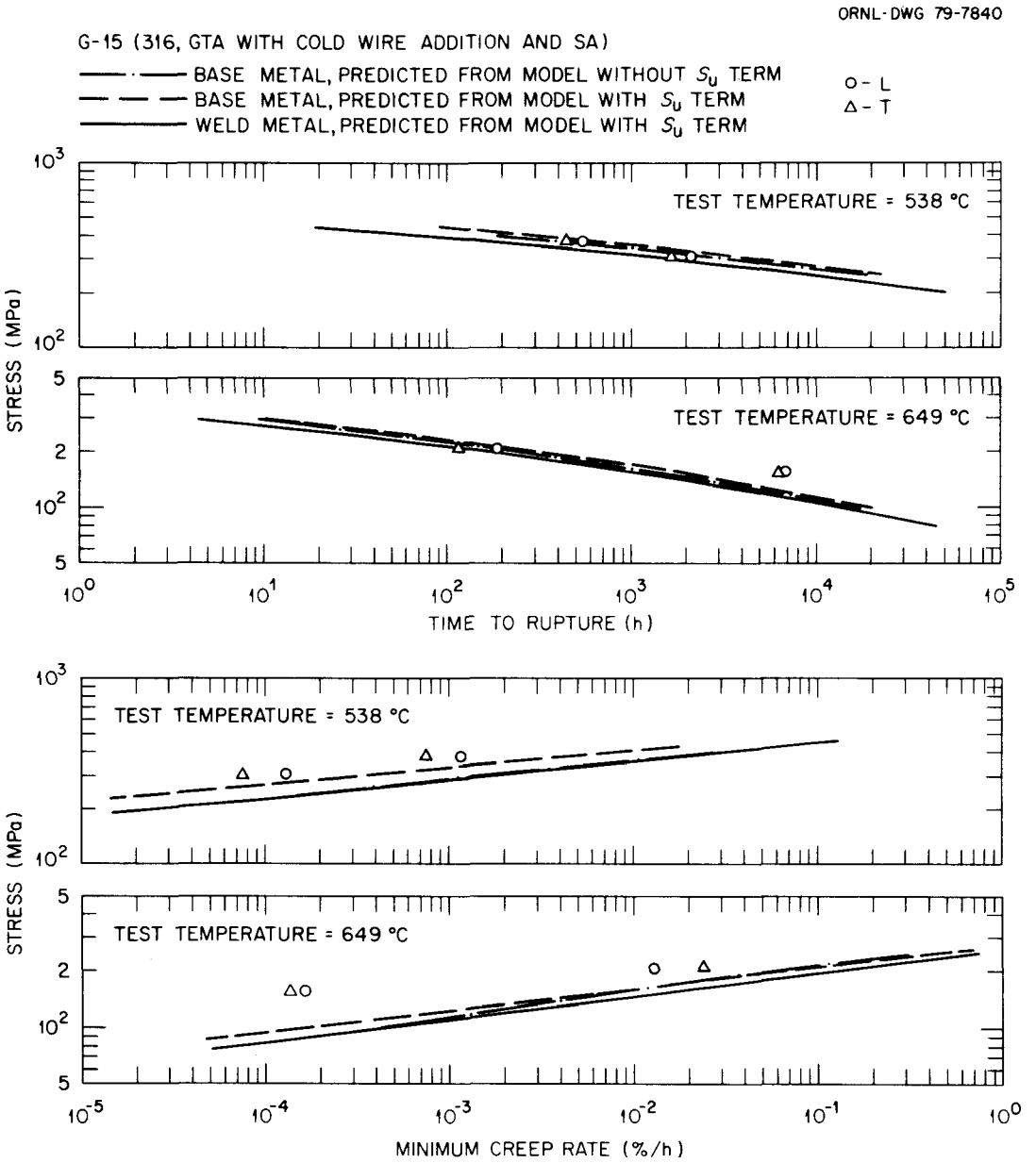

Fig. 24. Comparison of Experimental Time to Rupture and Minimum Creep Rate with Values Computed from Models with and without Elevated-Temperature S_u for Type 316 GTA Weld Metal and the Weldment Specimens Removed from Formed-and-Welded Pipe G-15 of Type 316 Stainless Steel (McEnerney and Sikka Data).

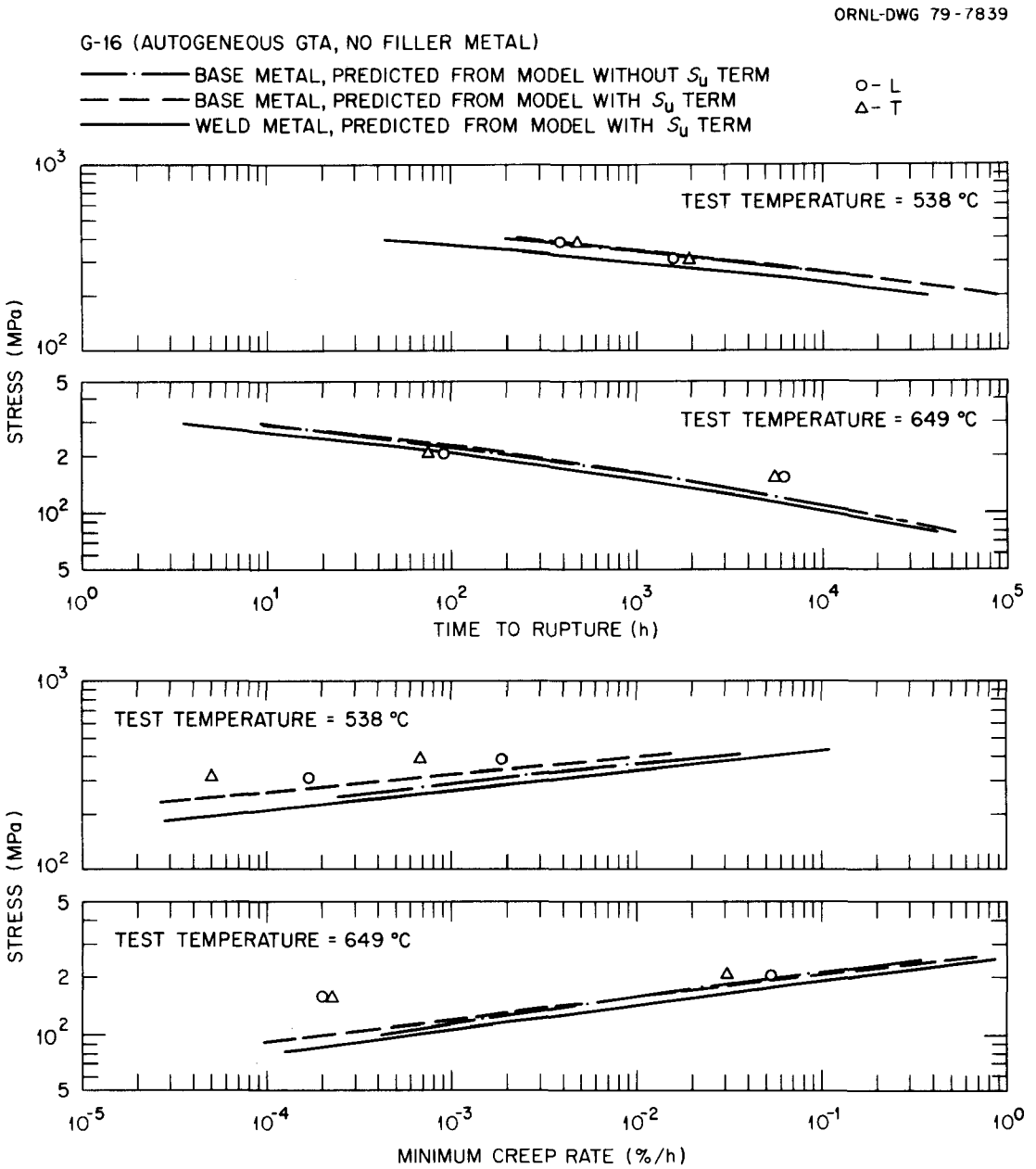

Fig. 25. Comparison of Experimental Time to Rupture and Minimum Creep Rate with Values Computed from Models with and without Elevated-Temperature S_u for Autogeneous GTA Weld Metal and Weldment Specimens Removed from Formed-and-Welded Pipe G-16 of Type 316 Stainless Steel (McEnerney and Sikka Data).

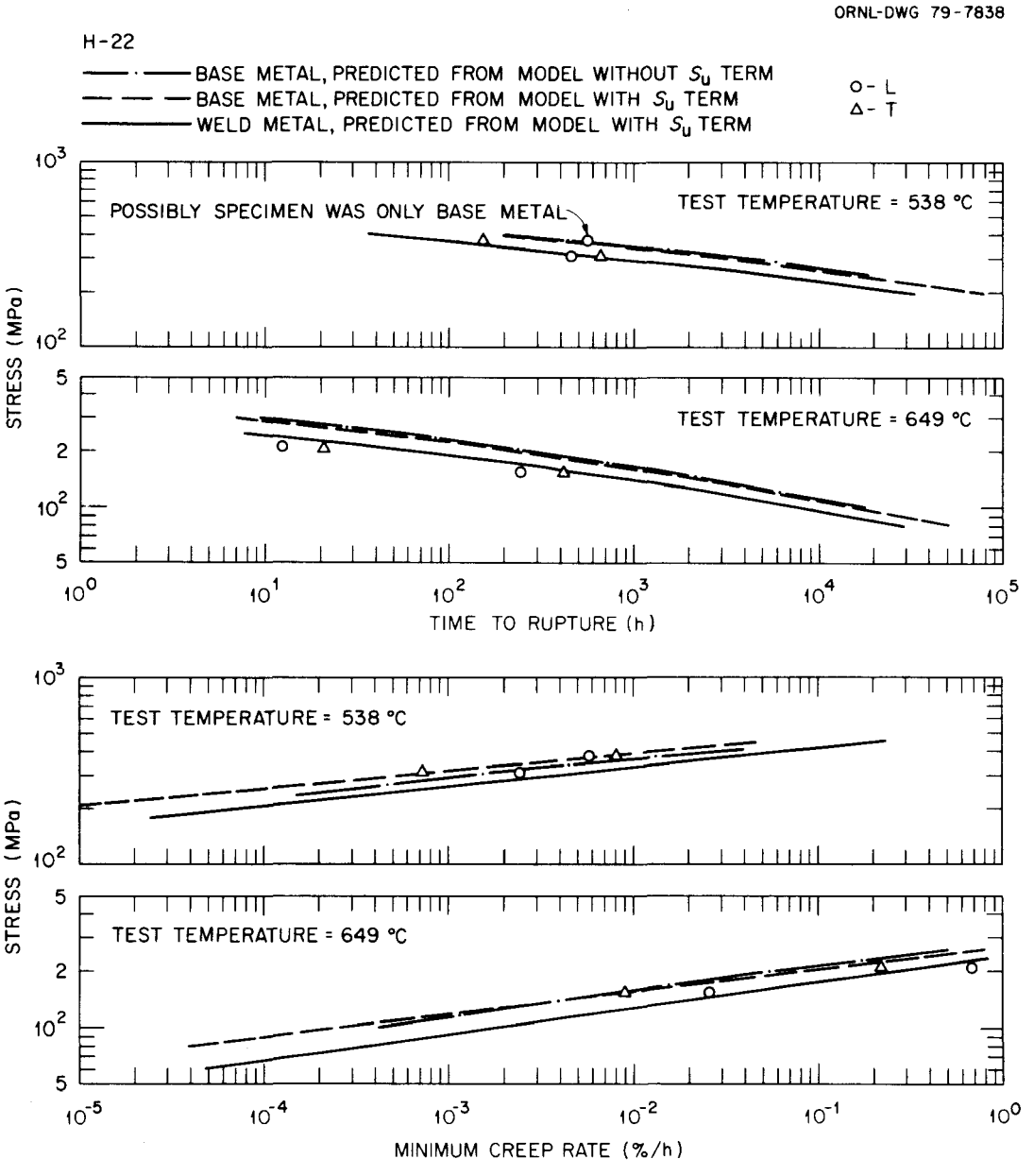

Fig. 26. Comparison of Experimental Time to Rupture and Minimum Creep Rate with Values Computed from Models with and without Elevated-Temperature S_u for 16-8-2 SA Weld Metal and Weldment Specimens Removed from Formed-and-Welded Pipe H-22 of Type 316 Stainless Steel (McEnerney and Sikka Data).

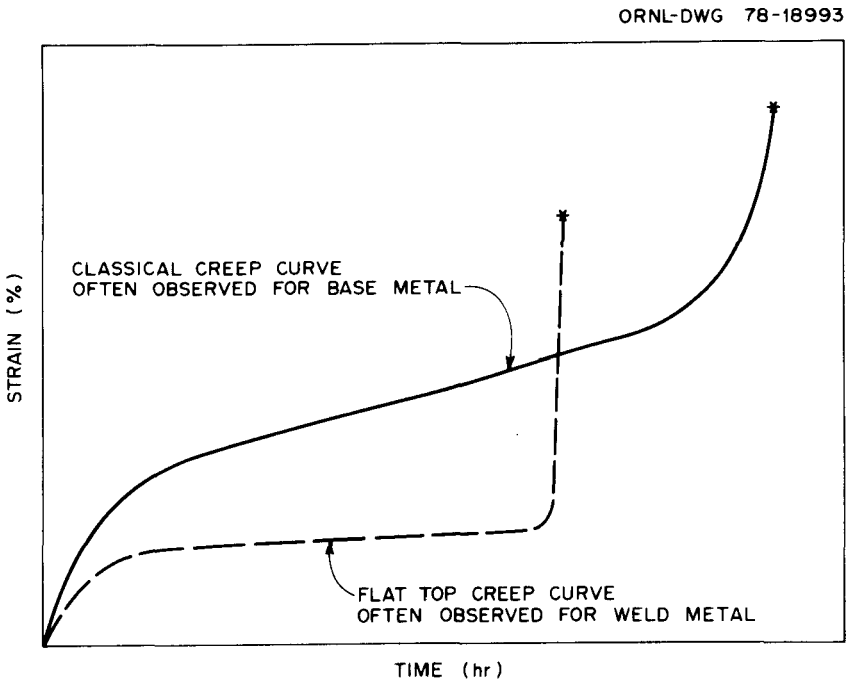

Fig. 27. Schematic Showing Classical Creep Curve Often Observed for Base Metal and Flat-Top Creep Curve Often Observed for Weld Metal Specimens.

Austenitic Stainless Steel Castings (McEnerney and Sikka,[13] Bolling et al.,[14] and Kanetoshi et al.[15] Data)

The cast metal data are included in this report to show their similarities to the weld metal properties. The data examined have the following characteristics:

McEnerney and Sikka[13] Data ("present investigation" in Figs. 28 and 29) — These data are on centrifugally cast pipe of type 316 stainless steel. The ferrite content of the pipe ranged from 15 to 23 FN. The specimens were tested in both the circumferential and axial directions. Details of chemical analysis, tensile and creep data, and microstructure of this pipe are available in ref. 13.

Bolling et al.[14] Data — These data are on two each centrifugally cast pipes of types 304 and 316 stainless steel. The ferrite content of the type 304 pipes ranged from 0.3 to 3.3 and from 10 to 15 FN. The nitrogen content of the type 304 pipes were 0.21 and 0.16%, respectively. The type 316 pipe had ferrite contents of 5 to 10 and 20 to 25 FN and nitrogen

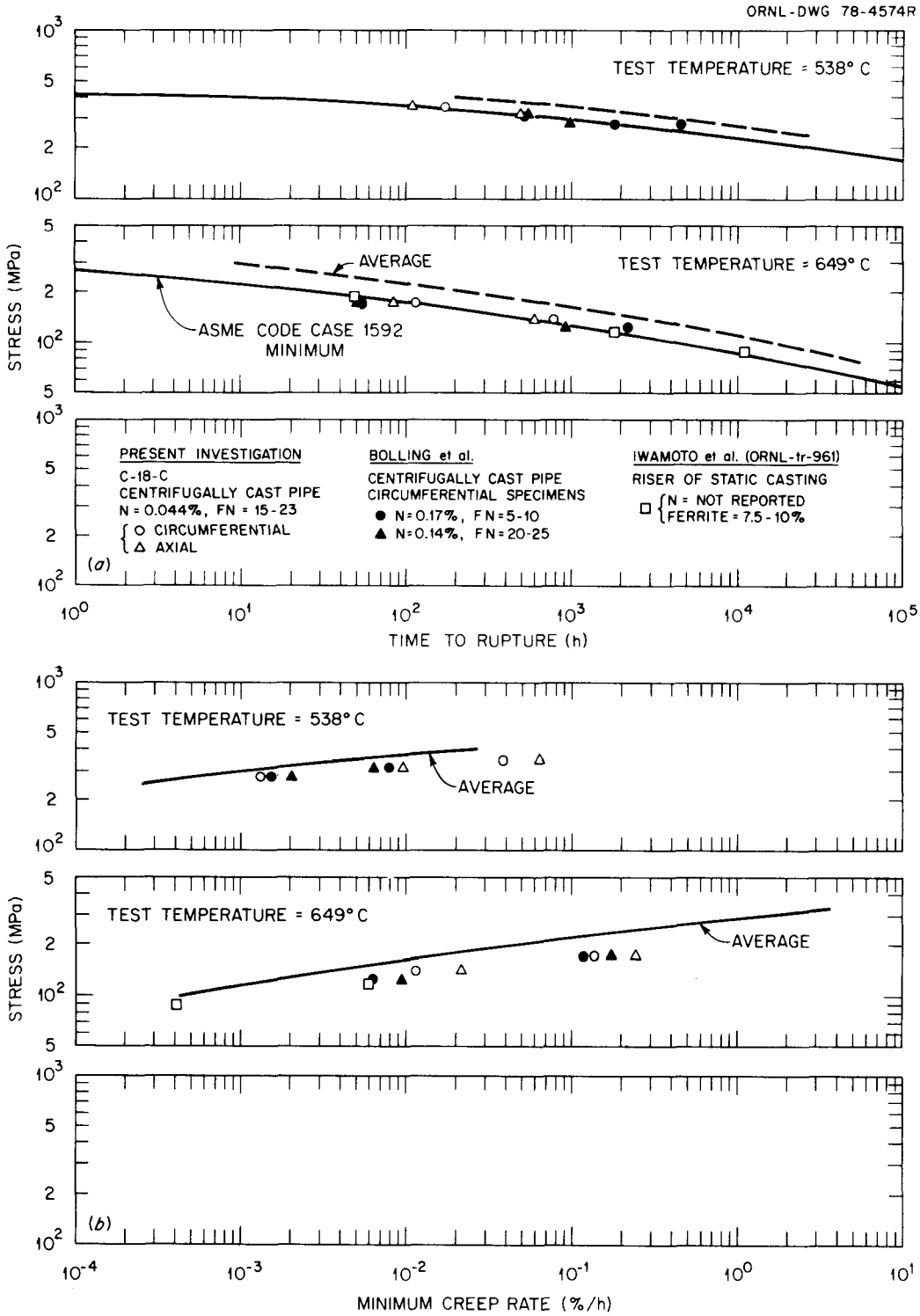

Fig. 28. Comparison of Experimental Time to Rupture and Minimum Creep Rate Data on Several Type 316 Stainless Steel Castings with the Average and ASME Code Case N-47 (Formerly 1592) Minimum Value Curves for the Wrought Material (McEnerney and Sikka, Bolling et al., and Iwamoto et al. Data).

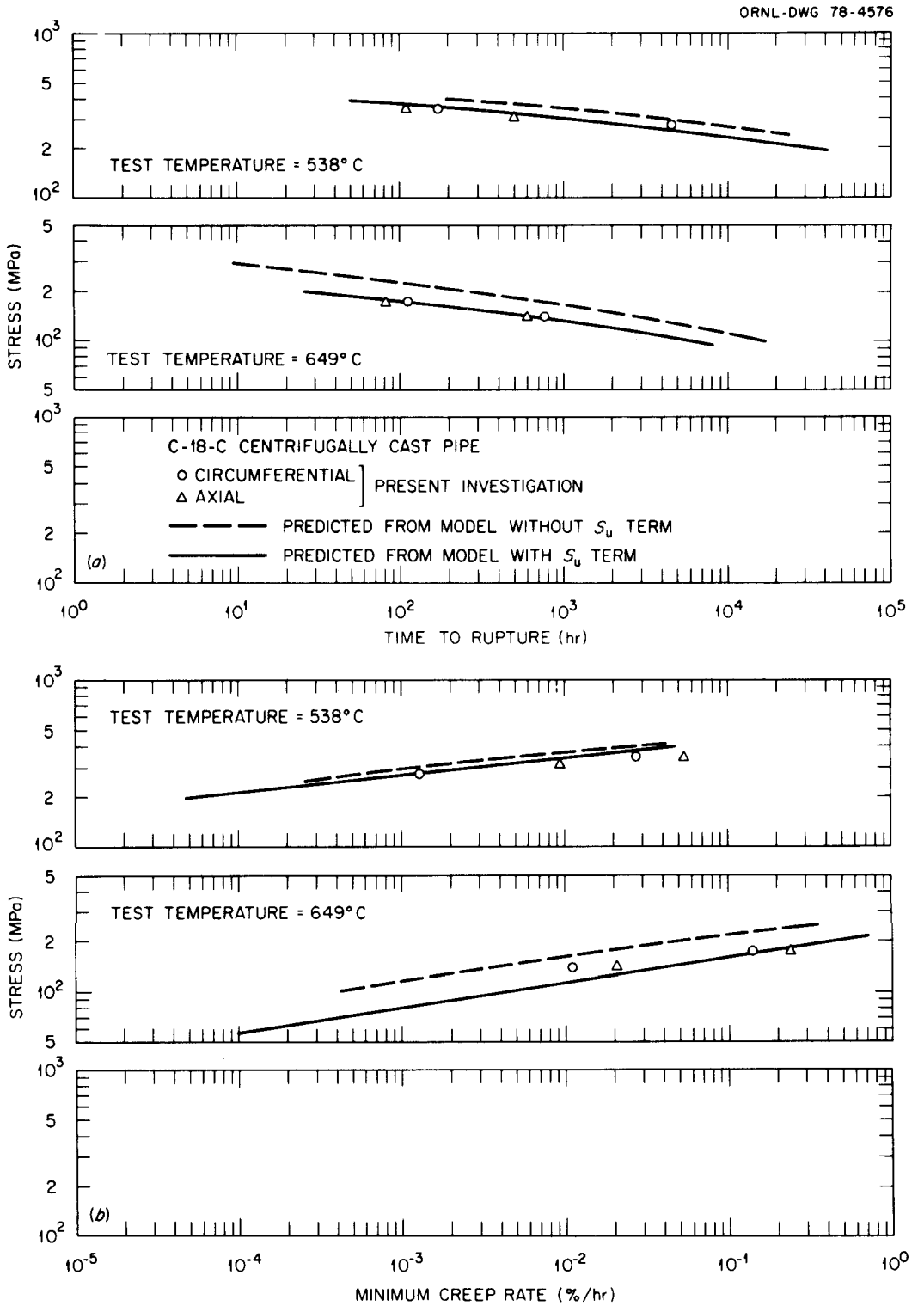

Fig. 29. Comparison of Experimental Time to Rupture and Minimum Creep Rate with Values Computed from Models with and without Elevated-Temperature S_u for the Centrifugally Cast Pipe of Type 316 Stainless Steel (McEnerney and Sikka Data).

content of 0.17 and 0.14%, respectively. The nitrogen contents of all pipes studied by Bolling et al. were much higher than the 0.044% present in pipes tested by McEnerney and Sikka.[13] The specimens were tested only in the circumferential direction.

Iwamoto et al.[15] Data — These data are for riser portions of a static casting. The casting contained 7.5 to 10% ferrite (note: not FN). Iwamoto et al. did not report the nitrogen content. Other details are available in ref. 15.

The time-to-rupture data from various type 316 castings are compared with the predicted average value curve for type 316 stainless steel base metal and the ASME Code Case N-47 minimum curve in Fig. 28(a). It should be noted that in all cases the as-cast rupture times were below the average for the wrought material. In fact, the rupture time coincided with or even fell below the ASME Code Case N-47 minimum curve for the wrought material. This behavior is similar to that observed for 16-8-2 submerged-arc welds made by B&W (Fig. 1).

The rupture times for the pipe studied by McEnerney and Sikka[13] were longer than those reported by Bolling et al.[14] This point is important to note because the pipes investigated by Bolling et al. had 0.14 to 0.17% N, compared with only 0.044% N in the pipe tested by McEnerney and Sikka. The ferrite contents for the pipes tested were essentially the same.

The rupture times for specimens taken from the risers of static castings[15] were similar to data obtained on centrifugally cast pipe. The minimum creep rates of all castings were above the average values for the wrought material [Figs 28(b)].

Figures 29 and 30 show that the S_u-based models can predict closely the t_r and $\dot{e}_m$ data of the centrifugally cast pipe and the t_r data of the static castings. The longest term test on the static casting exceeded 15,000 h.

The Bolling et al.[14] data on time to rupture and minimum creep rate for centrifugally cast pipes of types 304 and 316 stainless steel are compared with values computed from models with and without elevated-temperature ultimate tensile strength, S_u, in Figs. 31 through 34. The

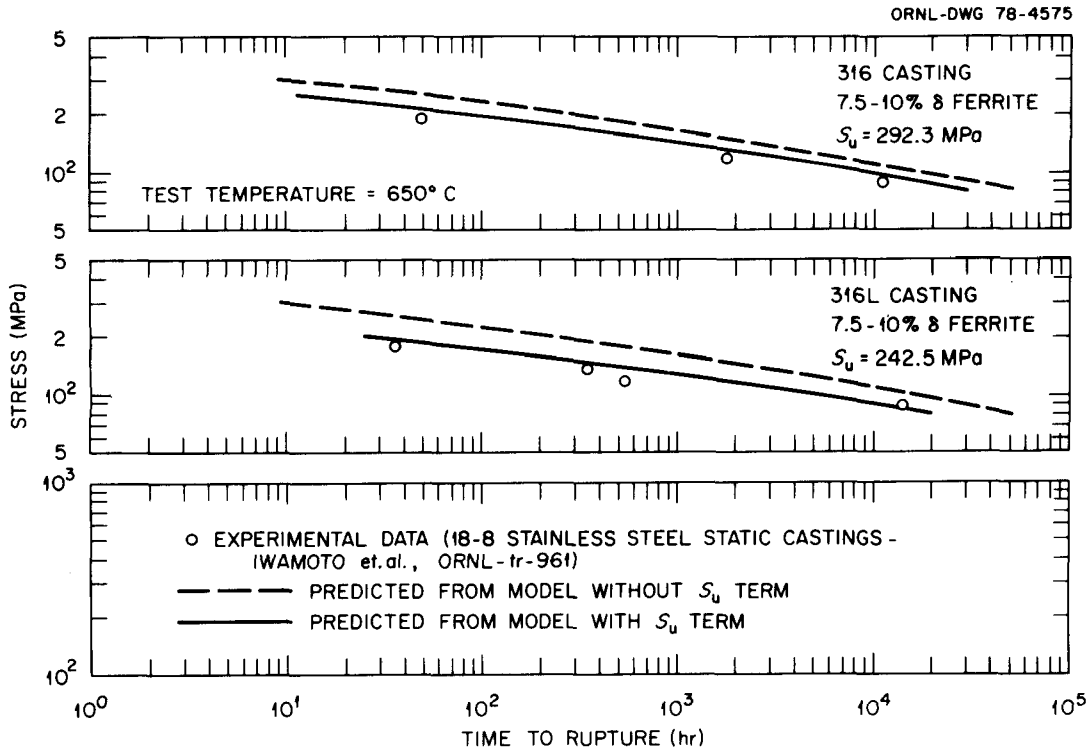

Fig. 30. Comparison of Experimental Time to Rupture with Values Computed from Models with and without Elevated-Temperature S_u for the Riser Portions of Static Castings of Types 316 and 316L Stainless Steel (Iwamoto et al.).

model without S_u gives an average curve for the wrought material. Note that the time to rupture for all four pipes is significantly below the average curve for the wrought material. The minimum creep rate also shows the same behavior except for the low-ferrite (CC4) type 304 cast pipe. Note also that the t_r and $\dot{e}_m$ data are predicted extremely well for all pipes except pipe CC4.

The chemical analyses and ferrite content of all four pipes were reported by Bolling et al.[14] Those data show that CC4 is the only pipe for which ferrite number varied from 0.3 to 3.3 FN (about an order of magnitude) and the nitrogen content varied from 0.21 (inner layer of pipe) to 0.14% (at the outer surface of the pipe). The other three pipes had relatively small variations in FN and nitrogen content. The large variation in FN and nitrogen content of pipe CC4 is probably responsible for the poor predictability of its creep behavior by the current models.

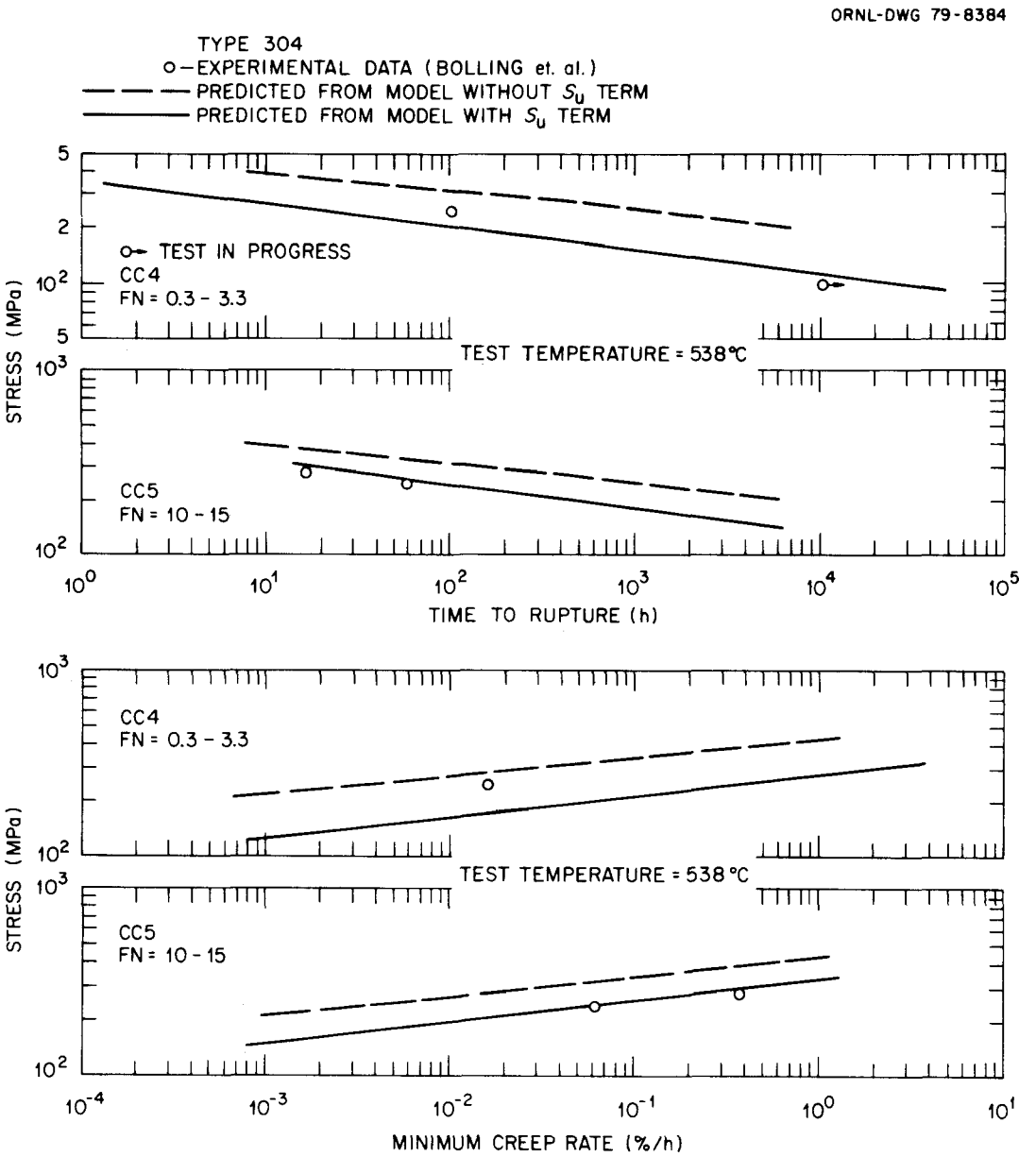

Fig. 31. Comparison of Experimental Time to Rupture and Minimum Creep Rate Data with Values Computed from Models with and without Elevated-Temperature S_u for Centrifugally Cast Pipes of Type 304 Stainless Steel at 538°C (Bolling et al. Data).

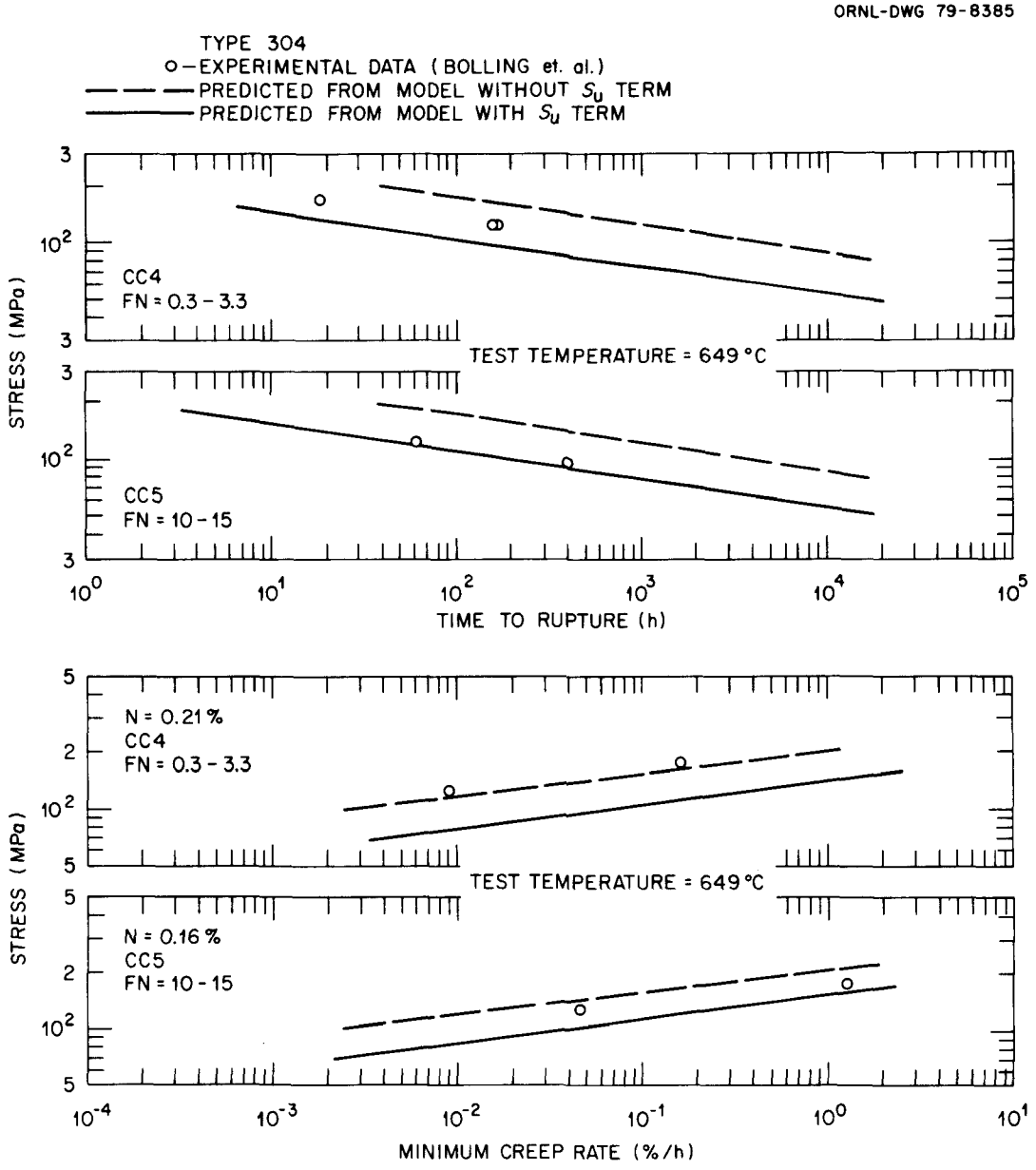

Fig. 32. Comparison of Experimental Time to Rupture and Minimum Creep Rate Data with Values Computed from Models with and without Elevated-Temperature S_u for Centrifugally Cast Pipes of Type 304 Stainless Steel at 649°C (Bolling et al. Data).

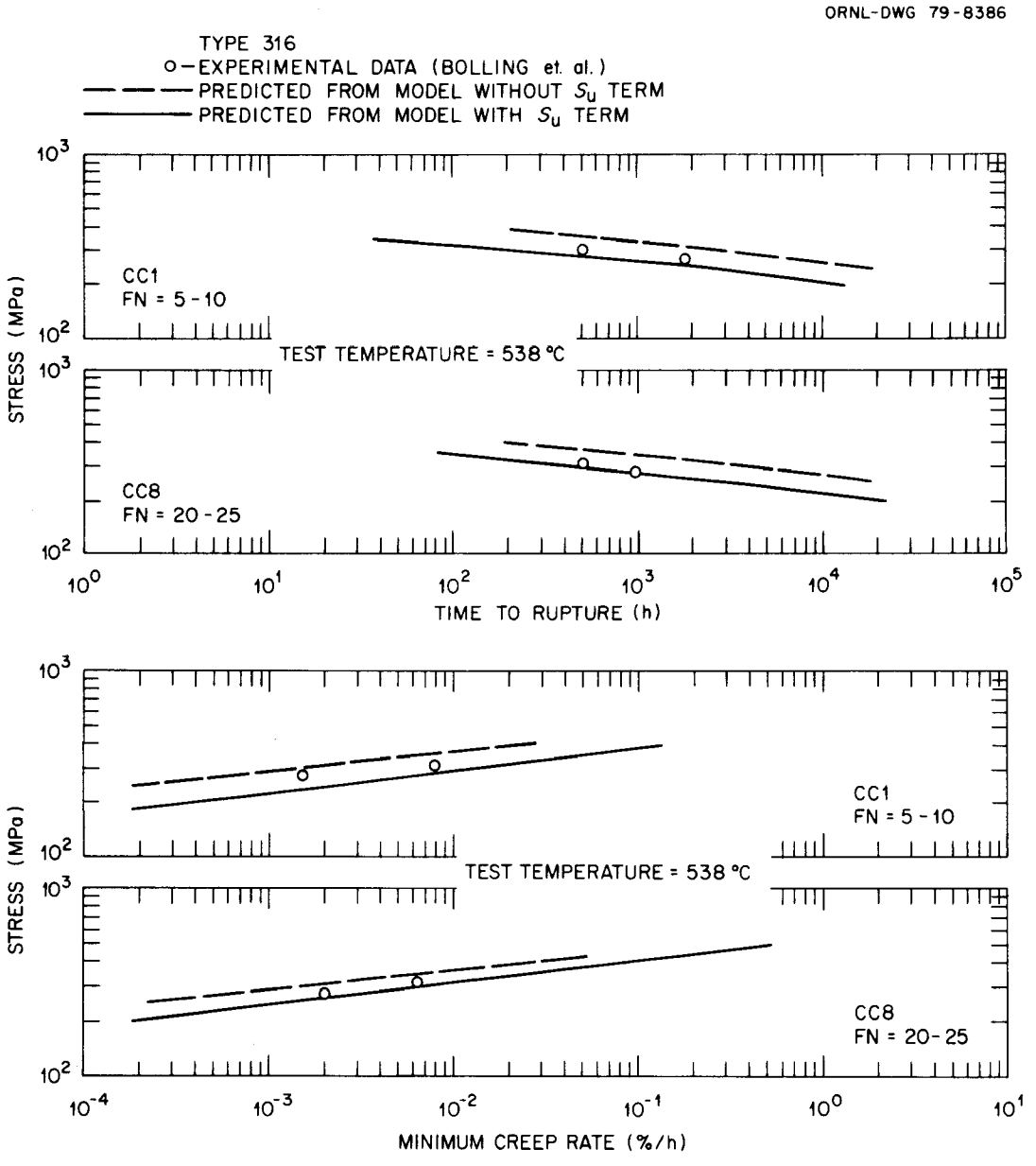

Fig. 33. Comparison of Experimental Time to Rupture and Minimum Creep Rate Data with Values Computed from Models with and without Elevated-Temperature S_u for Centrifgually Cast Pipes of Type 316 Stainless Steel at 538°C (Bolling et al. Data).

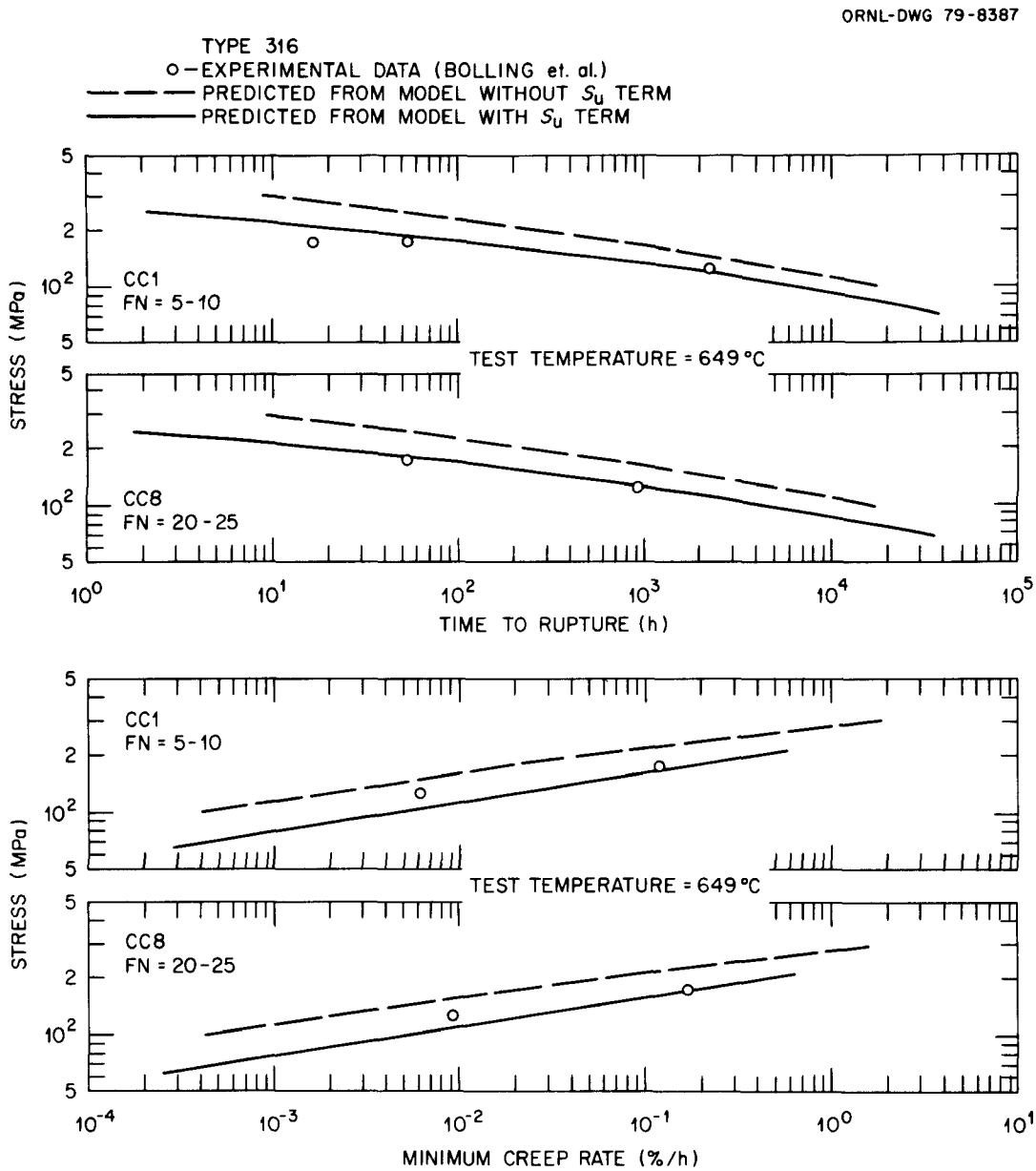

Fig. 34. Comparison of Experimental Time to Rupture and Minimum Creep Rate Data with Values Computed from Models with and without Elevated-Temperature S_u for Centrifugally Cast Pipes of Type 316 Stainless Steel at 649°C (Bolling et al. Data).

The creep specimens from the as-cast type 316 stainless steel pipe tested[13] at 649°C showed essentially zero ferrite number or, in other words, a complete transformation of ferrite to a nonmagnetic phase (most likely sigma). The 4500-h-long rupture test at 538°C also showed a significant drop in ferrite number. The optical microstructure of the as-cast and creep-tested specimens is shown in Figs. 35 and 36. These micrographs clearly show the transformation products in the ferrite islands. Note, however, that the transformation products are finer at 538°C and coarser at 649°C. Figure 35(c) shows that the creep-rupture in the transformed specimen may be occurring as a result of cracking in the transformed ferrite islands. Iwamoto et al.[15] identified by x rays the formation of sigma phase in their creep-tested specimens. Irrespective of transformation of δ-ferrite to sigma, the S_u model appears to predict closely the creep data of centrifugally cast pipes (Fig. 29) and the specimens taken from the risers of static castings (Fig. 30). These observations suggest that the creep behavior can be predicted when sigma phase forms during the creep test.

Cast-and-Worked Pipe Data After Ferrite to Nonmagnetic Phase Change Heat Treatment (McEnerney and Sikka[16] Data)

McEnerney and Sikka[16] have recently characterized a cast-and-worked pipe of type 316 stainless steel. This pipe (C-18F) contained ferrite corresponding to about 10 FN (measured on creep specimens) in the final fabricated conditions. Specimens from this pipe and a pipe section (C-17F), fabricated from the same heat with a different reduction sequence, were used to study the effect of ferrite-to-nonmagnetic transformation heat treatment. One set of specimens was cold strained 10% in an Instron testing machine before heat treatment at 800°C for 100 h. The ferrite number after this heat treatment was zero in both sets of specimens, so all the ferrite transformed into either austenite and sigma or only sigma phase (microstructures of these specimens are shown in Fig. 37). Tensile and creep tests were performed on these specimens at 538 and 649°C. Detailed data are available in another report.[16]

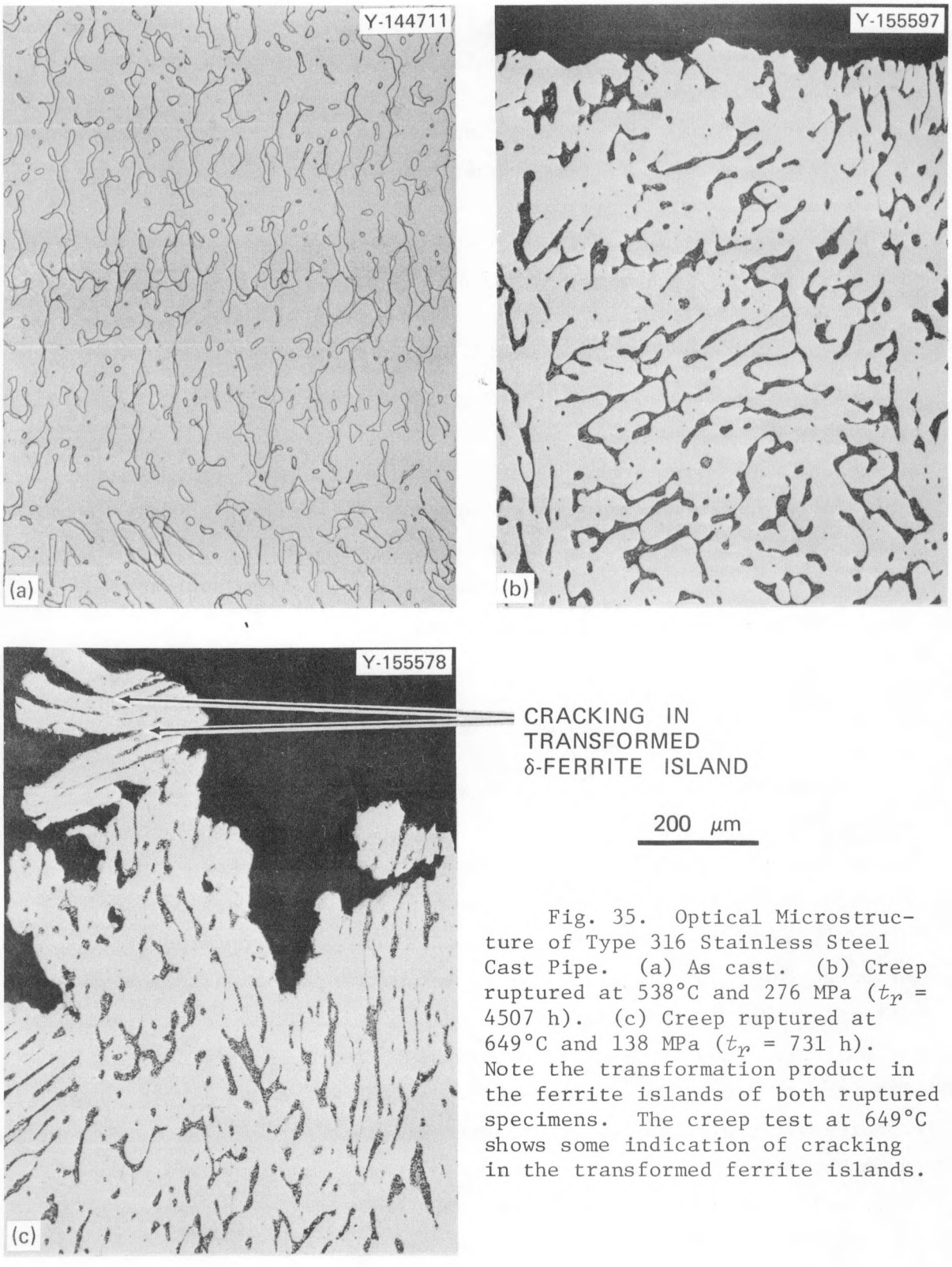

Fig. 35. Optical Microstructure of Type 316 Stainless Steel Cast Pipe. (a) As cast. (b) Creep ruptured at 538°C and 276 MPa (t_r = 4507 h). (c) Creep ruptured at 649°C and 138 MPa (t_r = 731 h). Note the transformation product in the ferrite islands of both ruptured specimens. The creep test at 649°C shows some indication of cracking in the transformed ferrite islands.

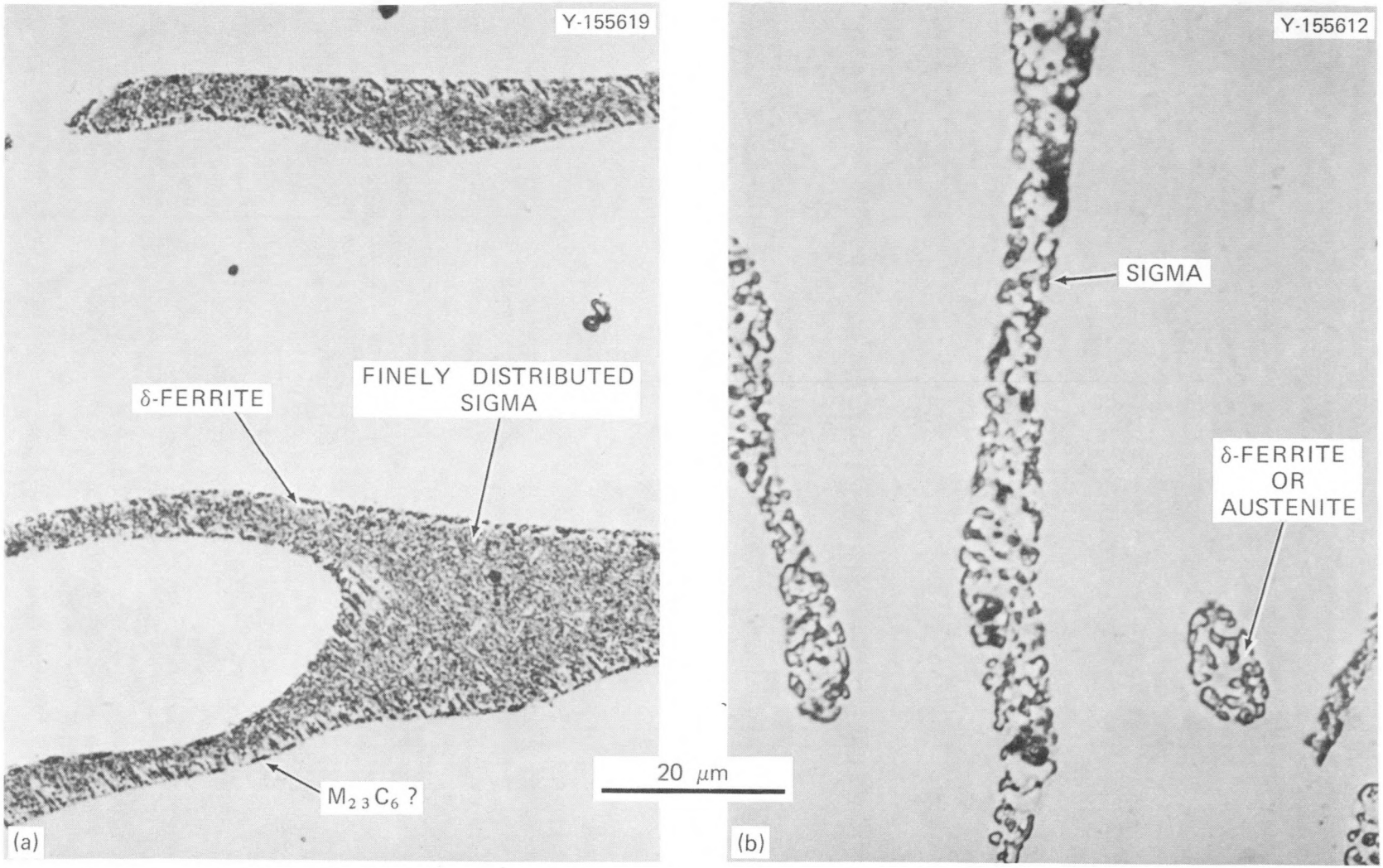

Fig. 36. High-Magnification Optical Micrographs of Creep Tested Specimens of Centrifugally Cast Pipe of Type 316 Stainless steel. Note the transformation products in δ-ferrite islands. (a) 538°C, 276 MPa, t_r = 4507 h. (b) 649°C, 138 MPa, t_r = 731 h.

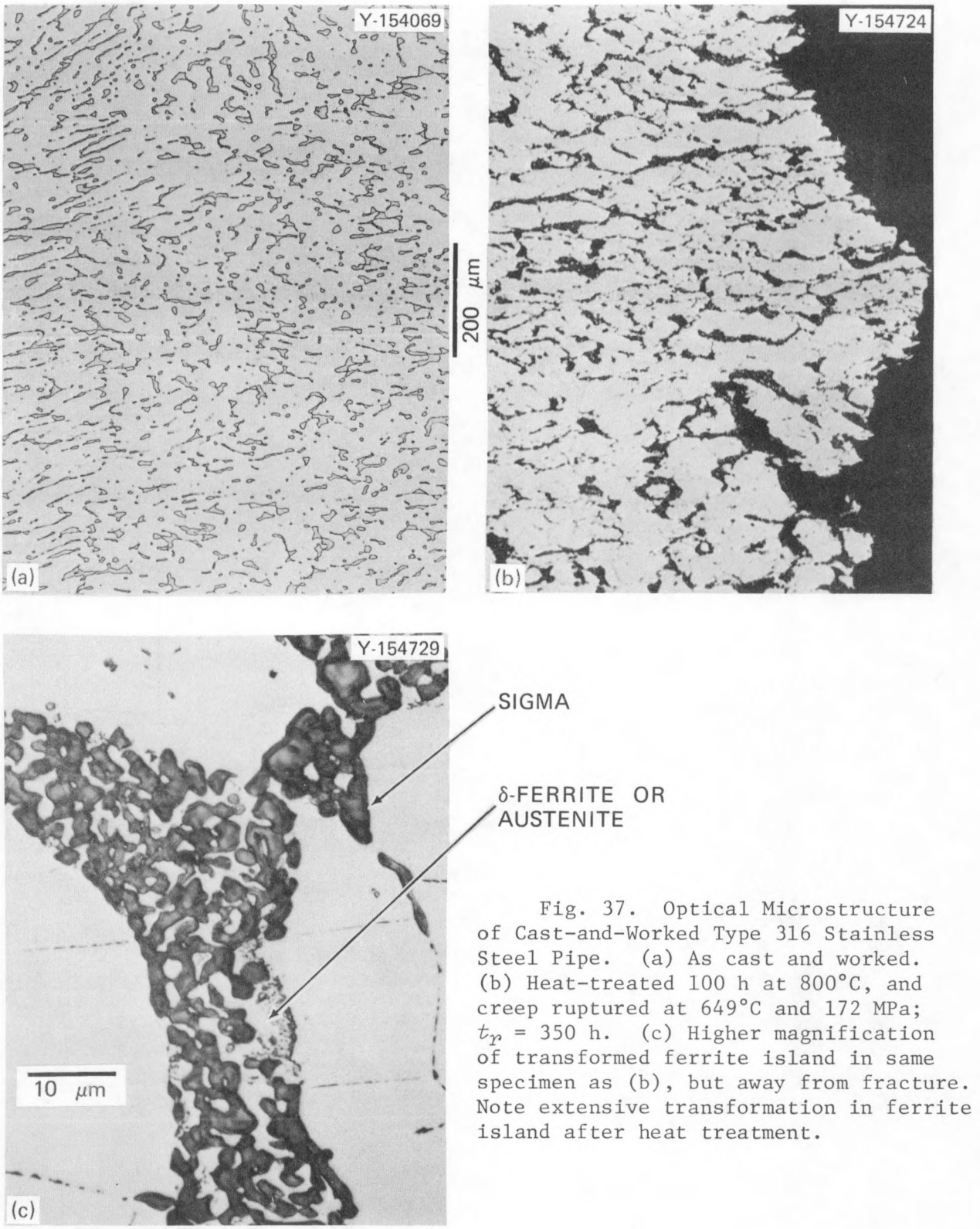

Fig. 37. Optical Microstructure of Cast-and-Worked Type 316 Stainless Steel Pipe. (a) As cast and worked. (b) Heat-treated 100 h at 800°C, and creep ruptured at 649°C and 172 MPa; t_r = 350 h. (c) Higher magnification of transformed ferrite island in same specimen as (b), but away from fracture. Note extensive transformation in ferrite island after heat treatment.

Figure 38 compares the experimental time to rupture and minimum creep rate with values computed from models with and without S_u. Note that both the t_r and $\dot{e}_m$ are closely predicted for these heat-treated specimens. Figure 37 shows the optical microstructure of specimens as cast and worked and after heat treatment and creep rupture. The micrographs show massive sigma phase particles in δ-ferrite islands after the 800°C 100-h treatment. The creep-ruptured specimen shows some indication of cracking in these transformed ferrite islands. This observation is similar to the micrographs shown in Fig. 35(c). It is important to note that 800°C 100-h heat treatment had transformed δ-ferrite to sigma phase. The formation of this phase prolonged t_r and lowered $\dot{e}_m$ (although failure appears to occur from cracking in the transformed δ-ferrite islands), and the results are still predictable by the current models. In predicting these results we used the elevated-temperature ultimate tensile strength values on the heat-treated specimens.

We showed in this section and the previous section that creep rupture data are predictable by the use of elevated-temperature ultimate tensile strength of the starting material, irrespective of whether sigma phase is formed at the start or during the creep test. However, it is important to note that the S_u for the model be obtained from material in the same condition as the creep specimen. For example, using S_u from material with prior sigma phase may predict to long t_r for untransformed material. This happens even when cracking is observed in transformed ferrite islands. These observations may imply that when ferrite is transformed to sigma in types 304 and 316 stainless steel the weakening effect due to cracking in the transformed regions is compensated for by the strengthening effect due to sigma being harder than δ-ferrite.

Use of Ultimate Tensile Strength as a Qualification Test

Once the predicting capabilities of current models are fully verified by more long-term data and accepted, they can be used along with the minimum stress-rupture data in the ASME Code Case N-47 to

determine the minimum ultimate tensile strength values required to assure that the weld metal properties equal or exceed the ASME Code Case minimum for the base metal. Such values of ultimate tensile strength have been computed for types 304 and 316 stainless steel with

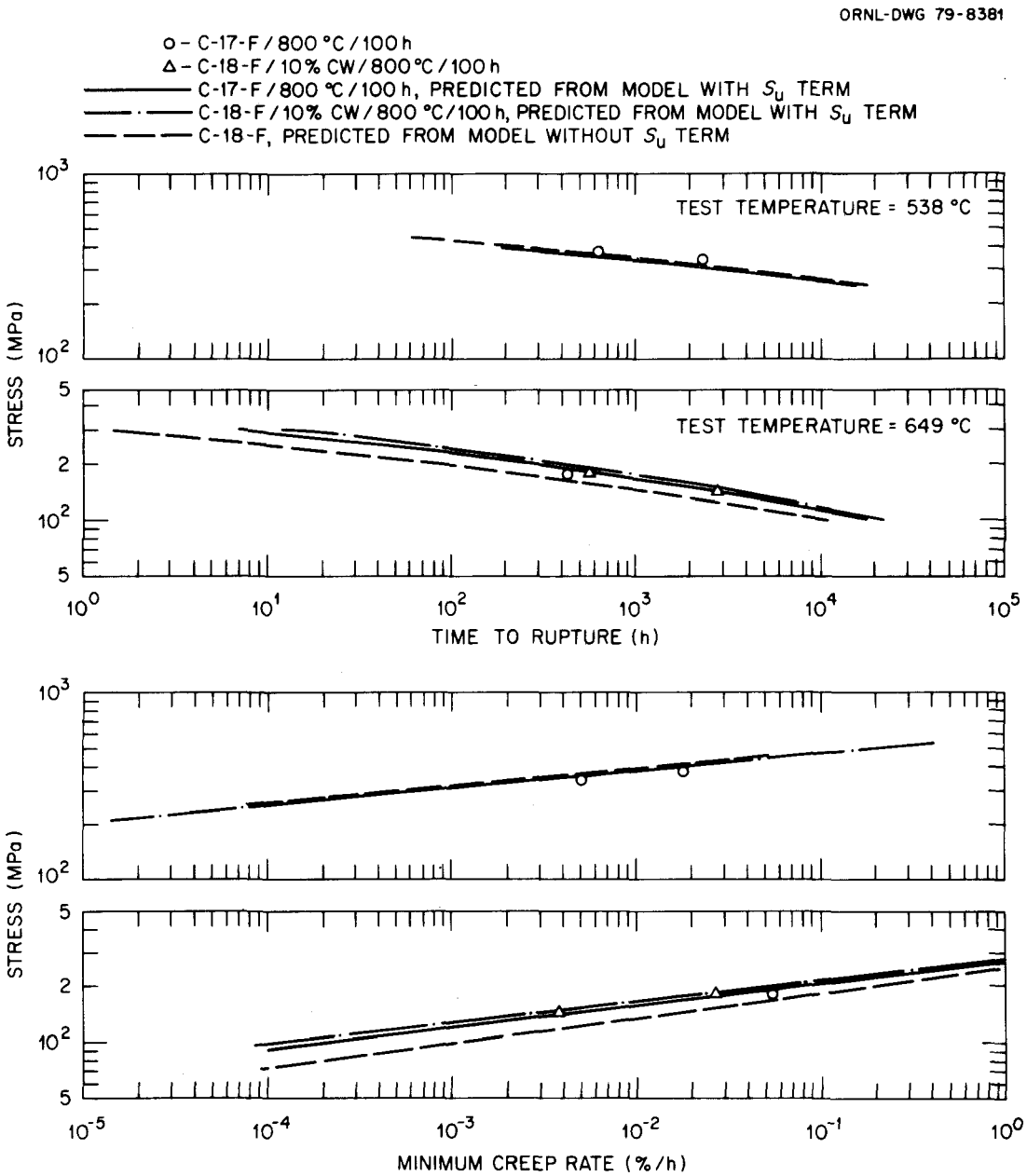

Fig. 38. Comparison of Experimental Time to Rupture and Minimum Creep Rate with Values Computed from Models with and without Elevated-Temperature S_u for Cast-and-Worked Pipes of Type 316 Stainless Steel. The C-17F pipe was given sigma heat treatment of 800°C for 100 h in the solution-annealed condition. The C-18F pipe was cold worked 10% before 800°C 100-h heat treatment (McEnerney and Sikka data).

Eqs. (3) and (7) along with 10^4-h minimum stress-rupture values from the ASME Code. These values are summarized in Table 2. According to results presented in the body of the report, the minimum values for types 304 and 316 stainless steel are expected to be applicable to weld metals of types 308 and 16-8-2.

Table 2. Calculated Elevated-Temperature Ultimate Tensile Strength Values Required to Meet ASME Code Case 1592 Minimum Stress-Rupture Curve

Test Temperature (°C)	Required Ultimate Tensile Strength, MPa (ksi)	
	Type 304[a]	Type 316[b]
538	361 (52.3)	402 (58.3)
593	300 (43.5)	304 (44.0)
649	241 (34.9)	252 (36.5)

[a]Values derived from type 304 model — should be applicable to type 308 weld metal.

[b]Values derived from type 316 model — should be applicable to type 16-8-2 weld metal.

Type 316 stainless steel is generally stronger than type 304 stainless steel and therefore the minimum ultimate tensile strength values for type 316 should have been higher than for type 304. However, Table 2 shows that the two values are essentially the same at the two higher temperatures, which is a consequence of the empirical nature of the current models. The values in Table 2 do imply that for the same value of ultimate tensile strength, type 16-8-2 is expected to be stronger than type 308. The validity of the values listed in Table 2 is confirmed by at least the short-term data on those weld metals and castings, which showed the minimum stress-rupture behavior.

It should be realized that some variation in elevated-temperature ultimate tensile strength is expected even when several specimens from the same material are tested. For example, 12 repeated tests[1] on type 316 stainless steel at 593°C showed a standard deviation of

±3.40 MPa in ultimate tensile strength values. Furthermore, the study[1] showed that ±2 standard deviation is required to describe total variation observed for 12 tests. Therefore, while using ultimate tensile strength as a qualification test, it may be possible to perform 3 tests and then use the average −2 standard deviations as the lowest possible value for the material in question.

It should also be noted that the tensile test strain rate has a strong effect on the ultimate tensile strength at elevated temperature, and therefore all data for current models should be obtained at a single strain rate of 8.33×10^{-5}/s. Predictions based on other strain rates will show poor agreement with the experimental data.

DISCUSSION

No models are available currently for welds except the isothermal (593°C) model developed by Ward and Blackburn[7] for the creep-rupture behavior of type 16-8-2 weld metal. We have shown that the previously developed[1,2] base metal models containing elevated-temperature ultimate tensile strength (S_u) for types 304 and 316 stainless steel can be applied to predict closely the rupture time and the minimum creep rate behavior of individual weld deposits of types 308 and 16-8-2 and the as-cast austenitic materials. It should, however, be noted that the predicted minimum creep rate behavior for several welds was off by almost an order of magnitude. Such a discrepancy was explained on the basis of flat-top creep curves, Fig. 27, often observed for the welds. These curves are significantly different from the classical creep curves observed for the base metal. It was also suggested that the predictability of current models will get poorer as the creep curves deviate from the ideal behavior. Work is planned in the near future to understand the flat-top creep curves observed for various weld metals.

The S_u-based models could predict closely the creep-rupture behavior of welds and castings after various heat treatments. The heat treatments include saturation treatment, "885°F embrittlement," and sigma treatment.

This report has presented sufficient data on a variety of welds and castings to show than an ultimate tensile strength at the creep test temperature can be used as an *index* for estimating the relative rupture time and the minimum creep rate behavior of welds and castings.

Previous workers[7,8] have shown that the control of the welding process and parameters through realistic engineering procedure specifications can yield welds with consistent time-dependent mechanical properties. Our results show that an elevated-temperature ultimate tensile strength could be used to check if indeed all the welding procedures were followed and that the welds meet the minimum specified properties.

Although the predicted values from rupture models containing elevated-temperature ultimate tensile strength describe the short-term data very well, we recommend that these models not be used to extrapolate beyond the range of available test times.

SUMMARY AND CONCLUSIONS

The creep data on various welds of types 308 and 16-8-2 stainless steel, centrifugally cast pipes, and static castings were compared with the rupture time and minimum creep rate values predicted from the previously published[1,2] base metal models with and without elevated-temperature ultimate tensile strength. From the similarities in chemical composition, we assumed that the type 304 models should be applicable to type 308 weld metal and type 316 models should be applicable to type 16-8-2 weld metal. The following conclusions can be drawn from this work:

1. Base metal models containing elevated-temperature ultimate tensile strength (S_u) can predict closely the rupture time and minimum creep rate of various weld deposits, centrifugally cast pipe, and the riser portions of static castings. The minimum creep rate of welds whose creep curves deviated significantly from the classical creep curves were predicted poorly.

2. The time to rupture was generally predicted more closely than the minimum creep rate.

3. The time to rupture and minimum creep rate could also be predicted when sigma phase was formed before or during creep testing of welds and castings.

4. Our results suggest that the elevated-temperature ultimate tensile strength can be used as an index for estimating the relative rupture time and minimum creep rate data of austenitic welds and castings.

5. It should be possible to use elevated-temperature ultimate tensile strength as a qualification test to check if the welding procedures are followed during fabrication and if the welds meet the minimum specified creep properties.

6. Although the predicted values from rupture models containing elevated-temperature ultimate tensile strength describe the short-term data very well, we recommend that these models not be used to extrapolate beyond the range of available test times.

REFERENCES

1. V. K. Sikka, M. K. Booker, and C. R. Brinkman, *Use of Ultimate Tensile Strength to Correlate and Estimate Creep and Creep-Rupture Behavior of Types 304 and 316 Stainless Steel,* ORNL-5285 (October 1977).
2. M. K. Booker, *Mathematical Analysis of the Elevated-Temperature Creep Behavior of Type 304 Stainless Steel,* ORNL/TM-6110 (December 1977).
3. W. R. Simmons and J. A. Van Echo, *Report on the Elevated-Temperature Properties of Stainless Steels, ASTM Data Ser. Publ.* DS 5 S1, American Society for Testing and Materials, Philadelphia, 1965.
4. R. T. King, D. P. Edmonds, and E. Bolling, "Status of Testing on 16-8-2 Submerged-Arc Welds," *Mechanical Properties Test Data for Structural Materials Quart. Prog. Rep. Oct. 31, 1976,* ORNL-5237, pp. 150–53.
5. "Case N-47," pp. 105–231 in *Code Cases, Boilers and Pressure Vessels,* 1977 ed., American Society of Mechanical Engineers, New York, 1977 (and supplementary revisions).

6. R. T. King, N. C. Cole, R. G. Berggren, and G. M. Goodwin, "Properties and Structure of 16-8-2 Stainless Steel Weld Metal," paper ASME 75-PVP-45 presented at the Second National Congress on Pressure Vessels and Piping, San Francisco, June 23–27, 1975.
7. A. L. Ward and L. D. Blackburn, "Creep and Rupture Behavior of Weld-Deposited Type 16-8-2 Stainless Steel at 593°C," *J. Eng. Mater. Technol.* 99: 159–67 (April 1977).
8. A. L. Ward, *Austenitic Stainless Steel Weld Materials — A Data Compilation and Review*, HEDL/TME-74-25 (May 1974).
9. R. L. Klueh and D. A. Canonico, "Elevated-Temperature Tensile Properties and Microstructure of a Weld-Overlaid Type 304 Stainless Steel Forging," pp. 113–40 in *Elevated-Temperature Properties of Austenitic Stainless Steels*, American Society of Mechanical Engineers, New York, 1974.
10. R. L. Klueh and D. A. Canonico, *The Creep-Rupture Properties of a Weld-Overlaid Type 304 Stainless Steel Forging*, ORNL-5085 (February 1976).
11. J. W. McEnerney and V. K. Sikka, *Characterization of Time-Independent Properties of Formed-and-Welded Pipes for Breeder Reactor Application*, ORNL/TM-6609 (in press).
12. J. W. McEnerney and V. K. Sikka, *Time-Dependent Properties of Rolled and Welded Pipes*, report in preparation.
13. J. W. McEnerney and V. K. Sikka, *Characterization of Three Developmental Centrifugally Cast-and-Worked Austenitic Stainless Steel Pipes*, report in preparation.
14. E. Bolling, G. M. Goodwin, J. P. Hammond, R. L. Klueh, and R. T. King, *Properties and Structure of CPF8 and CPF8M Centrifugally Cast Pipe*, report in preparation.
15. K. Iwamoto et al., "On the High-Temperature Strength of 18-8 Mo Stainless Steel Castings," *Zairyo* 14(137): 101–10 (1965); ORNL-tr-961.
16. J. W. McEnerney and V. K. Sikka, *Effect of Sigma Heat Treatment on Tensile and Creep Properties of Type 316 Stainless Steel*, report in preparation.

Blank Page

ORNL/TM-6781
Distribution
Category
UC-79b, -h, -k

INTERNAL DISTRIBUTION

1–2. Central Research Library
3. Document Reference Section
4–5. Laboratory Records Department
6. Laboratory Records Department, RC
7. ORNL Patent Section
8. J. J. Blass
9. M. K. Booker
10. C. R. Brinkman
11. J. A. Clinard
12. J. M. Corum
13. J. R. DiStefano
14. D. P. Edmonds
15. G. M. Goodwin
16–18. M. R. Hill
19. J. F. King
20. W. J. McAfee
21. H. E. McCoy
22–31. J. W. McEnerney
32. C. E. Pugh
33. A. F. Rowcliffe
34–43. V. K. Sikka
44. G. M. Slaughter
45. J. H. Smith
46. R. W. Swindeman
47. G. T. Yahr
48. R. W. Balluffi (consultant)
49. A. L. Bement, Jr. (consultant)
50. W. R. Hibbard, Jr. (consultant)
51. E. H. Kottcamp, Jr. (consultant)
52. M. J. Mayfield (consultant)
53. J. T. Stringer (consultant)

EXTERNAL DISTRIBUTION

54–55. DOE DIVISION OF REACTOR RESEARCH AND TECHNOLOGY, Washington, DC 20545

Director

56. DOE OAK RIDGE OPERATIONS OFFICE, P.O. Box E, Oak Ridge, TN 37830

Assistant Manager, Energy Research and Development

57–318. DOE TECHNICAL INFORMATION CENTER, Office of Information Services, P.O. Box 62, Oak Ridge, TN 37830

For distribution as shown in TID-4500 Distribution Category, UC-79b (Fuels and Materials Engineering Development); UC-79h (Structural Materials Design Engineering); and UC-79k (Components).